Sampling terrigenous diffuse sources in watercourse: Influence of land use and hydrological conditions on dissolved organic matter characteristics

Amine Boukra, Matthieu Masson, Corinne Brosse, Mahaut Sourzac, Edith Parlanti, Cécile Miège

Title. Sampling terrigenous diffuse sources in watercourse: influence of land use and hydrological conditions on dissolved organic matter characteristics.

Amine Boukra[1], Matthieu Masson[1], Corinne Brosse[1], Mahaut Sourzac[2], Edith Parlanti[2], Cécile Miège[1]

[1] INRAE, RiverLy, F-69625, Villeurbanne, France

[2]Univ. Bordeaux, CNRS, Bordeaux INP, EPOC, UMR 5805, F-33600 Pessac, France

Correspondence to: matthieu.masson@inrae.fr ; +33472208706; RiverLy, INRAE, 5 rue de la Doua, Villeurbanne, France, 69625

Highlights:

- This study addresses the sampling of non-point sources of DOM in watercourses
- A combination of land use markers discriminated DOM terrigenous signature in streams
- Hydrological conditions impacted the signature of watercourse DOM
- New indicators from HPSEC/UV-fluorescence improved the study of DOM composition

Abstract

Diffuse and point sources of dissolved organic matter (DOM) in streams influence its composition, interactions and fate in the aquatic ecosystem. These inputs can be very numerous at the scale of a watershed, and their identification remains a challenge especially in the case of diffuse sources related to land use. The complexity of the transfer mechanisms and the reactivity of DOM throughout the soil-water column continuum raise questions about the sampling of diffuse sources in watercourses. To answer this question, we compared the characteristics of soil-extracted DOM influenced by a particular land use (homogenous sub-catchment of forest and vineyard) and DOM collected from the watercourse adjacent to the soil samples. A 28-day incubation experiment of soil extracts was designed to remove the labile fraction of DOM. During the first 3 days, between 40 and 70 % of the DOC mass was lost for both types of soils. A set of optical indicators (UV-Visible, EEM fluorescence and HPSEC/UV-fluorescence) showed that the labile fraction was mostly composed by low (<1 kDa) and high (>10 kDa) protein-like molecules. At the end of the incubation, soil-extracted DOM was mainly composed of medium molecules (1-10 kDa) associated to terrigenous humic-like compounds. Its optical and size molecular signature tended towards that in the adjacent watercourses and was specific to land use. However, the characteristics of DOM in watercourses was also influenced by the hydrogical conditions, probably due to a transfer of top soil DOM during high water periods and both deep soil and autochtonous DOM during low water periods. These results were obtained by a set of indicators including novel ones derived from high-pressure size exclusion chromatography (HPSEC/UV-fluorescence). Finally, this study demonstrated that it is possible to sample the DOM representative of a land use directly in the river downstream of the homogeneous sub-basin by multiplying the samples during contrasting hydrological conditions.

Keywords: Dissolved organic matter; non-point sources; land-use; optical fingerprint

1 Introduction

Dissolved organic matter (DOM) is a complex set of organic compounds operationally defined as material obtained after water filtration (commonly ranging from 0.2 to 0.7 µm) (Zsolnay, 2003; Zark and Dittmar, 2018) with an average molecular size distribution that ranges from <100 Da to >100000 Da (Nebbioso and Piccolo, 2013; Hawkes et al., 2019). DOM plays a major role in environmental biogeochemistry, particularly as the main driver of terrestrial carbon to the aquatic environment, as a substrate for the growth of microorganisms (Bolan et al., 2011; Mladenov et al., 2022), but also in the fate and bioavailability of pollutants (Reuter and Perdue, 1977; Aiken, 2014). At the scale of a watershed, DOM inputs to the rivers can originate from a wide range of natural and anthropogenic sources (Nebbioso and Piccolo, 2013). These sources can be either point sources (e.g. wastewater treatment plants and storm overflows) or diffuse discharges (e.g. terrigenous inputs related to land use, underground inputs, autochthonous production; Carstea et al., 2020; Williams et al., 2016).Point discharges of DOM can be easily located and their sampling is often representative of these sources. For example, DOM from wastewater treatment plant discharges, constitutes a mixture of organic molecules including microbial degradation products, surfactants, pharmaceutical products, phytosanitary products (herbicides, fungicides, insecticides) and disinfection by-products (Michael-Kordatou et al., 2015; Verkh et al., 2018).

Diffuse sources of DOM are more difficult to locate and study due to the complexity of geochemical interactions, degradation processes and the uncontrolled meteorological events at the origin of these DOM sources. In the case of terrigenous contributions of diffuse DOM sources, studies have shown that the soil type governs the amount of DOM transferred to the aquatic downstream environment (Bolan et al., 2011). Organic type soils discharge more DOM than mineral type soils. Land use as well as soil biomass influence the composition of DOM transferred to the watercourse (Kalbitz et al., 2003). This could be explained by the fact that

DOM is considered to be the most active and labile part of soil organic matter (Guigue et al., 2014).Low molecular weight labile compounds make up the organic matter in the surface layers of the soil. Their proportion decreases in depth soils giving way to higher fraction of refractory compounds of high molecular weight. In addition, the hydrology of the watershed, or more specifically, the direction of water flow along the soil, determines the type of organic matter transferred to rivers. Indeed, Sanderman et al., 2009 demonstrated that vertical flow would favor the transfer of the more refractory denatured organic matter, whereas lateral flow would transfer labile organic matter characteristic of the surface soil layers. However, establishing DOM fingerprints in rivers related to land uses and occupations, driven hydrology, is a complex task. The high reactivity of DOM labile fraction coupled with environmental conditions and the nature of the soils make difficult the establishment of reliable DOM fingerprints. Here we define a DOM fingerprint as a set of physico-chemical markers calculated from one or several analytical techniques (e.g. optical characteristics, molecular size distribution), which are relevant to discriminate a given source. At present, classically used techniques such as UV-Visible spectroscopy and excitation emission matrix (EEM) fluorescence have brought major advances in the study of chromophoric and fluorescent DOM. The application of these spectroscopic techniques has allowed, for example, to differentiate between types of DOM depending on the sources and the state of evolution (Li and Hur, 2017). Another analytical technique that showed relevance to characterize DOM composition, is the size exclusion chromatography (HPSEC). The principle of HPSEC is based on the separation of molecules according to their size or hydrodynamic volume. Previous studies have shown that HPSEC can be used to determine the distribution of molecular weight for DOM by calculating indicators used to characterize polymers such as average molecular weight (Mw), number average molecular weight (Mn) and polydispersity (p) (Huang et al., 2021). Detection by diode arrays and fluorescence (HPSEC/UV-fluorescence) allowed to specifically target absorbing and

fluorescent compounds in organic matter, providing further qualitative information on the size continuum of DOM molecules (Asmala et al., 2021; Brezinski and Gorczyca, 2019). However, the combined information of molecule size and type, provided by HPSEC/UV-fluorescence, could be further explored to propose relevant indicators improving DOM fingerprints. In this context, the aim of this paper was to determine the representativeness of sampling a terrigenous diffuse source of DOM in watercourses. More precisely, we studied the link between soil-extracted DOM, characterized by a particular land use, and DOM collected in the soil-adjacent watercourse. A second objective was to improve the study of DOM optical fingerprints by introducing new indicators from size exclusion chromatography HPSEC/UV-fluorescence.

To achieve this, the characteristics of i) DOM extracted from soils defined by distinct land use (forest and vineyard), and ii) DOM from adjacent watercourses collected during high and low water periods were compared. . The starting hypothesis is that during the high water period, there would be a greater contribution of the terrigenous source. This comparison was performed by characterizing DOM properties using a combination of optical analysis techniques including UV-Visible spectrophotometry, EEM fluorescence spectroscopy and HPSEC/UV-fluorescence.

2 Materials and methods

2.1 Site description

All sampling areas were located in Ardière-Morcille watershed (152 km^2) in eastern France. The catchment area, in its downstream part, is characterized by vineyard activities representing more than 32 % of total landscape (Peyrard et al., 2016). Other land uses such as forests (37 %) and pastures (21 %), are also present in the upstream watershed (Figure 1).

The region's climate is semi-continental with a mean annual rainfall of 940 mm and episodic snowfalls during winter (Gouy et al., 2021). The soils are mostly sandy and erodible and the geological characteristics are an altered hercynian crystalline basement of mostly porphyric biotite granite. The watershed is characterized by very steep slopes, ranging between 5 and 30-35 % favoring surface runoff. In addition, numerous and fast hydrological events make the riverbed, rarely dry (Rabiet et al., 2015).

2.2 Sampling design and samples preparation before experimentations in laboratory

Water samples were collected manually from rivers, downstream of 10 homogenous sub-catchment areas characterized by 5 forest land occupations and 5 vineyard land uses (Figure 1). Sub-catchment land uses were determined based on Corine Land Cover 2018 using Qgis 3.14 software. Sampling was carried out during two campaigns: A first sampling campaign in January 2021 during a period of high water (3.65 and 0.2 $m^3.s^{-1}$ respectively for Ardières and Morcille Rivers) and a second sampling campaign in July 2021 during the period of low water (0.65 and 0.03 $m^3.s^{-1}$ respectively for Ardières and Morcille Rivers). The flow data was obtained at Villié-Morgon and Beaujeau stations located downstream of the Ardières and Morcille rivers. The water samples were collected in 250 mL borosilicate glass bottles previously cleaned by an automatic washer at 90°C, then calcined in an oven at 500°C. The samples were filtered in the field using polypropylene syringe and polyvinylidene fluoride (PVDF) filters with a

132 porosity of 0.45 µm. The filtrate was first used to rinse the 250 mL borosilicate glass bottle
133 three times before filling them completely. The samples were then stored in a cooler (at ± 4°C)
134 protected from light during their transport to the laboratory, then stored at 4°C in the dark until
135 analysis. Experimental blanks using ultrapure water (resistivity at 18.2 MΩ.cm) were prepared
136 in laboratory using the same protocol as in the field, in order to identify possible contamination
137 due to bottles, syringes or filters.

138 Soils were sampled in the forest and vineyard sub-catchment areas upstream of water samples
139 (radius of 30 to 50 m) during the high water sampling campaign. Detailed geographic
140 coordinates are available in supplementary material 1. In each site, 20 cm of top soils were
141 taken with an auger; four subsamples were randomly selected to collect approximately 1 kg of
142 soil. Each subsample was placed in a polypropylene bag. Once all 4 subsamples were collected,
143 the bulk sample was mixed in the bag. The 10 soil samples were stored at 4°C protected from
144 light until preparation in the laboratory where the soils were sieved with a 2 mm stainless steel
145 sieve, placed in aluminum trays (40x60 cm) and dried for 96 h at 40 °C in an oven.

146 To summarize, for each sub-catchment area, one water sample was collected during high water
147 period as well as one soil sample (composite of 4 randomly collected subsamples). During low
148 water periods, an additional water sample was collected.

149 **2.3 Dissolved organic matter extracted from soils (soil extracts)**

150 Dissolved organic matter was extracted from soil samples by stirring 20 g (dry weight) of soil
151 in 200 mL of ultrapure water with 10 mM $CaCl_2$ (Supplementary Material 2). Stirring was
152 performed at 180 rotations per minute in a Lovibond thermoregulator cabinet at 20 °C in dark
153 condition. After 6 h of agitation, the samples were centrifuged at 4500 g during 15 min and the
154 supernatant was filtered through 0.45 µm (PVDF filter). An initial 60 mL sample was collected
155 before the incubation experiment.

2.4 Incubation experiment

Two inoculums of forest and vineyard soils were prepared 48 h before the incubation experiment. To obtain better microbial diversity, both forest and vineyard inoculums were prepared from, respectively, a mixture of the 5 forest soils and the 5 vineyard soils (Kalbitz et al., 2003; Guigue et al., 2014). For each inoculum, 5 g of the 5 corresponding soil samples were added to 200 mL of ultrapure water. These preparations were then shaken at 20° for 48h in the dark. A nutrient solution of $(NH_4)_2SO_4$ and KH_2PO_4 (C:N:P:S:K molar ratio of <5:1:1:1:1) was also prepared 1h prior to the incubation. The addition of nutrients allows optimizing the activity of the microorganisms during the following incubation.

Incubation of DOM extracted from soils was performed by adding 35 µL of inoculum and 1 mL of nutrient solution to the samples immediately after the soil DOM extraction step (Guigue et al., 2014) (Supplementary Material 2). Controls without inoculum nor nutrient solution (inoculum blanks) and controls without soil extracted DOM (extraction blanks) were performed. All samples and controls were incubated at 20°C in the dark, with continuous shaking at 180 rotations per minute during 28 days. The incubation period of 28 days was chosen based on previous work that studied the time required to degrade the labile fraction of DOM from soil samples (Guigue et al., 2014). Sub-samples at 3, 7, and 14 days of incubation were collected to monitor changes in DOM quantity and quality (optical properties).

2.5 Analytical strategy

2.5.1 Dissolved organic Carbon

Dissolved organic carbon (DOC) analyses were performed by high temperature catalytic combustion according to the standard NF EN 1484 and using an Analytik Jena multi N/C® 3100 TOC analyzer. The calibration, rinsing, quality controls solutions, as well as samples, were introduced in precombusted (at 500°C during 2 h) glass vials, where they were acidified

180 to pH=1 with hydrochloric acid (HCl 37% RPE). The detection limit was 0.2 $mgC.L^{-1}$ and the
181 analytical uncertainty was 12%. The accuracy of the analyses (105%) was routinely checked
182 using a certified standard of potassium hydrogen phthalate (5 $mg.L^{-1}$, Fluka®) different from
183 that used for the calibration (0.2–25 mgL^{-1}, Sigma-Aldrich®).

184 **2.5.2 UV-Visible spectroscopic analysis**

185 UV-Visible spectroscopy analyses were performed using a Shimadzu UV 1900
186 spectrophotometer with a 1 cm path length quartz cell (Hellma Analytics®). Absorbance
187 spectra were acquired between 200 and 800 nm with a resolution of 1 nm and a scan speed of
188 0.2 $s.nm^{-1}$. A baseline correction was carried out using an ultrapure water blank over the same
189 wavelength range. A series of classical descriptive indicators ($SUVA_{254}$, absorbance ratios and
190 spectral slopes) were calculated from the generated absorbance spectra (Table 1).

191 **2.5.3 EEM fluorescence spectroscopy and PARAFAC decomposition**

192 Excitation-emission matrix (EEM) fluorescence analyses were performed using an Aqualog
193 (Horiba Scientific) spectrofluorometer in a 1 cm path length quartz cuvette (Hellma
194 Analytics®) thermostated at 20°C. The Aqualog instrument was equipped with a 150 W Xenon
195 arc lamp and excitation wavelengths were scanned using a double-grating monochromator from
196 240 to 800 nm at 5 nm intervals, while the emission spectra were obtained using a high-gain
197 CCD detector at intervals of approximately 0.58-nm (1-pixel) for wavelengths from 240
198 to 800 nm. All EEM spectra were corrected for instrumental biases and normalized to the area
199 under the Raman peak of water, at 350 nm excitation, acquired daily. Fluorescence intensities
200 are therefore expressed in Raman units (R.U). In order to avoid inner filter effects, all samples
201 with maximum absorbance > 0.1 were diluted. Raman and Rayleigh scattering peaks were
202 removed by subtracting blank spectrum. The generated spectra were treated using TreatEEM-
203 V1 software developed by Dario Omanović (Ruđer Bošković Institute, Zagreb, Croatia;

https://sites.google.com/site/daromasoft/home/treateem). The fluorescence indices HIX (Zsolnay), BIX, FI, YFI (Table 1) were calculated for an excitation wavelength of 250, 310, 370 and 280 nm respectively (Heo et al., 2016; Huguet et al., 2009; Mcknight et al., 2001; Zsolnay et al., 1999)

The multi-way parallel factor analysis (PARAFAC) was applied to a set of 103 EEM spectra (corresponding to 83 soil extracts and 20 water samples collected from the adjacent streams). The PARAFAC model was run, using the drEEM toolbox under MatLab R2020a, for 4 to 8 components with non-negativity constraints (Murphy et al., 2013). Four components were validated based on split-half analysis and compared to previously reported components using the OpenFluor fluorescence database.

2.5.4 Size exclusion chromatography HPSEC/UV-fluorescence

High performance size exclusion chromatography (HPSEC; LC-2030C 3D Plus, Shimadzu) coupled with photodiode array (Deterium D2 Lamp PDA) and fluorescence (RF-20A xs) detectors was used to determine the molecular size distribution of DOM. The injection volume was 10 µL with a flow rate at 0.8 $mL.mn^{-1}$ of phosphate buffer mobile phase (NaCl, KH_2PO_4 and K_2HPO_4). Two columns (Shodex OHpak SB-803 HQ, Shodex OHpak SB-802 HQ) coupled in series were used for the chromatographic separation. The first column covered an exclusion range between 1 kDa and 100 kDa and the second one between 0.2 kDa and 1 kDa. Analytical standards PSS (polysulfonate) were used as references of average molecular weights (0.246, 1.6, 4.3, 6.8, 10, 17, 32, 77 kDa). Other standards were also used to cover a wider range of molecule types, such as nitrates (0.063 kDa), Bovin Serum Albumin BSA (66 kDa) and Polyacrylic Acid PAA standards (1, 2.6 and 3.6 kDa). A calibration curve of molecular weight (from 0.2 - to 77 kDa) according to elution volume was calculated using these analytical standards (Brezinski and Gorczyca, 2019).

The UV-DAD detector allowed the acquisition of chromatograms on an absorbance range between 200 and 450 nm with an increment of 1.2 nm every 300 ms. Regarding the fluorescence detector, 3 couples of excitation-emission wavelengths (Ex-Em) were retained for all the analyses The fluorescence intensities were measured for the wavelengths corresponding to the humic-like components (315-443 nm), protein-type components (280-330 nm), and tryptophan-type components (278-354 nm) were measured every 400 ms.

To optimize the use of the data generated by HPSEC/UV-fluorescence, a Gaussian decomposition was performed. The aim was to decompose the size continuum obtained in each HPSEC chromatogram into distinct Gaussian components (Eq. 1). For this, the toolbox «peakfit.m » (O'Haver, 2020) was applied on MatLab *R2020a*.

Eq. 1 : $$A(x;\mu;\sigma;\varphi) = \sum_{i=0}^{nC} \varphi_i e^{\frac{-(x-\mu_i)2}{2\sigma^2 i}} + \varepsilon$$

where nC is the number of Gaussian components, ε is the residuals which represent the variability not taken into account by the model, x is the peak area, μ is the peak position parameter (elution volume), σ is the peak width and φ is the proportion of each fitted Gaussian distribution.

The number of detected components was validated using the Bayesian Information Criterion (Asmala et al., 2021). Areas of the identified Gaussian components were summed in order to calculate the total sec absorbance (TSA) from chromatograms obtained with detection at UV 254 nm (Asmala et al., 2021). The total sec fluorescence TSF was calculated from chromatograms obtained with fluorescence detection at three excitation-emission (Ex-Em) wavelengths (nm): Ex: 315-Em: 443, Ex: 280-Em: 330 and Ex: 278-Em: 354. These wavelengths are classically used to characterize DOM properties (Table 1). The calibration

curve allowed classifying each Gaussian component in a molecular weight fraction, based on the peak position (elution volume). In this study, three molecular weight fractions were defined as: low molecular weight fraction (LMW) with an average molecular weight < 1 kDa, medium molecular weight fraction (MMW) with an average molecular weight ranging from 1 to 10 kDa, and high molecular weight (HMW) with an average molecular weight >10 kDa. The LMW, MMW and HMW fractions represent the relative percentages of respectively small, medium and large molecules detected at the measured wavelengths.

2.6 Mathematical and statistical analyses

Anova analysis coupled with a Tukey test (packages stats and rstatix; R 4.0.2 software) were used to compare both forest and vineyard soil extracts, the temporal kinetics of the incubation study and also for the comparison between soil extracts and adjacent natural waters for all UV-Vis, EEM fluorescence and HPSEC/UV-fluorescence indicators. Principal component analysis (PCA;package factoextra, R 4.0.2 software) was also used for the comparison of soil extracts vs. natural adjacent waters, and a linear discriminant analysis (LDA; packages MASS and klaR, R 4.0.2 software) for the selection of the most relevant DOM markers of forest and vineyard soil occupations.

3 Results

3.1 Dissolved organic carbon

Before incubation, dissolved organic carbon (DOC) concentrations (Figure 2.A) in the 5 forest soil extracts ranged from 22.7 to 48.2 $mg.L^{-1}$ with a mean value of 32.7 ± 9.4 $mg.L^{-1}$. For the 5 vineyard soil extracts, DOC concentrations varied between 16.14 and 34.14 $mg.L^{-1}$ with a mean value of 23.8 ± 6.6 $mg.L^{-1}$. These values are consistent with those obtained in previous studies (Rinot et al., 2021). No significant difference (Tukey test, $p > 0.05$, n=50) in DOC concentrations was found between forest and vineyard soil extracts before incubation.

The percentage of DOC (Figure 2.B) was calculated for the duration of the experiment (28 days). For forest soil extracts, the percentage of DOC decreased by 67 ± 8 %, with a significant decrease (Tukey test, $p < 0.05$, n=50)) of 42 ± 9 % within the first three days of incubation. For vineyard soil extracts, the percentage of DOC decreased by 61 ± 3 %, with a significant decrease of 46 ± 5%, again during the first three days of incubation. Previous studies showed DOC losses range from 5 to 93% depending on soil types (forest, pasture, arable) and extraction protocols (pressurized hot-water, water extraction, leaching extraction) (Guigue et al., 2014; Kalbitz et al., 2003).

DOC concentrations of samples collected in streams adjacent to forest soils ranged from 2.2 to 3.0 $mg.L^{-1}$ during high water periods (Figure 2.A). For these same sites, DOC concentrations were significantly higher (Tukey test, $p < 0.05$, n=20) ranging between 3.3 $mg.L^{-1}$ and 4.6 $mg.L^{-1}$ during low water periods. In the streams adjacent to vineyard soils, DOC ranged from 3.1 to 4.4 $mg.L^{-1}$ during high water. Non-significant difference was observed during low water periods with DOC concentrations ranging between 3.5 and 4.6 $mg.L^{-1}$. In addition, DOC concentrations were significantly higher in the vineyard stream samples than in the forest stream samples only during high water.

3.2 UV-Visible

UV-Visible spectra (Supplementary Material 3) show a classical pattern, i.e. an exponential decrease between 200 and 250nm, followed by a slight decrease between 250 and 400 nm. Then the signal is close to the background for wavelength superior to 400 nm. A decrease in absorption is observed between the soil extracts before and after 28 days of incubation, at wavelengths from 250 to 400 nm, i.e. the range classically used to characterize the chromophoric DOM. $SUVA_{254}$ (Table 1) increased significantly (Tukey test, $p < 0.05$, n=50) over the 28-day incubation period of the experiment, from 0.98 ± 0.11 to 2.02 ± 0.12 $L.mg^{-1}cm^{-1}$ for forest soil extracts, and from 1.44 ± 0.45 to 3.02 ± 0.51 $L.mg^{-1}cm^{-1}$ for vineyard soil extracts (Figure 3.A). A significant difference (Tukey, test, $p < 0.05$, n=50) was observed between forest and vineyard soils only after the 3rd day of incubation. During the first 3 days, spectral slope $S_{275-295}$ and E2.E3 index (Table 1) values decreased significantly (Tukey test, $p < 0.05$, n=50) and then stabilized during the rest of the incubation period (Figure 3.B, C). Overall, values of $S_{275-295}$ for forest and vineyard extracts respectively decreased from 0.023 ± 0.002 to 0.017 ± 0.001 and from 0.022 ± 0.003 to 0.017 ± 0.003;andthe E2.E3 index values decreased from 7.60 ± 0.47 to 6.33 ± 0.59 and from 6.86 ± 0.92 to 5.91 ± 0.90,. The values of the SR, E2.E4 and E3.E4 (Table 1) ratios did not vary significantly between the soil extraction and the last day of the experiment (Figure 3.D, E, F).

Regarding samples collected in adjacent streams, no significant difference was observed according to land use. However, the indicator SR showed significant differences between high water and low water sampling periods (Tukey test, $p < 0.05$, n=20). Indeed, values of SR varied between 0.751 ± 0.0497 to 0.808 ± 0.012 and 0.775 ± 0.027 to 0.833 ± 0.011 for both forest and vineyard adjacent water samples. Previous studies on soil extracts and stream water samples (Sanderman et al., 2009; Liu et al., 2021; Chen et al., 2021) have reported UV-Visible index values in the same ranges as those presented in this work.

3.3 EEM fluorescence spectroscopy

The humification index (HIX; Table 1) showed a significant increasing trend during the first days of incubation (Tukey test, $p < 0.05$, n=50). These values stabilized for vineyard soil extracts while they decreased for forest soil extracts at the end of incubation (Figure 4.A). Indeed, the values increased from 3.1 ± 1.0 to 3.7 ± 1.5 for the forest soil extracts and from 2.9 ± 0.4 to 6.6 ± 0.7 for the vineyard soil extracts. Therefore, a significant difference (Tukey test, $p < 0.05$, n=50) is also observed between the two types of soils at the end of the experiment. No particular trend was observed for the indicator of biological activity (BIX; Table 1) and the Freshness index (FI; Table 1) during the incubation period (Figure 4.B, C). BIX values ranged from 0.71 ± 0.08 to 0.79 ± 0.08 for forest soil extracts; and from 0.63 ± 0.05 to 0.67 ± 0.02 for vineyard soil extracts; FI values from 1.40 ± 0.06 to 1.42 ± 0.04 for forest soil extracts; and from 1.31 ± 0.08 to 1.36 ± 0.04 for vineyard soil extracts. The YFI indicator (Table 1), showed a decrease according to incubation time (Figure 4.D). This decrease, however, is very limited for both soil extracts during the incubation experiment (YFI values from 0.89 ± 0.27 to 0.71 ± 0.06 and from 0.74 ± 0.04 to 0.61 ± 0.04 respectively for forest and vineyard soil extracts).

For water samples, only HIX showed a significant difference between water collected during high and low water (Tukey test, $p< 0.05$, n=20). HIX values varied between 8.44 ± 0.88 and 7.28 ± 1.11 for the streams adjacent to the forest, sampled during high and low water periods. For vineyard streams, it varied between 9.05 ± 0.34 and 7.39 ± 0.53 during the two sampling periods. The other indices BIX, FI and YFI showed no significant differences between forest and vineyard waters, nor between sampling periods. Values of fluorescence indices in this work are consistent with previous studies obtained on forest soils, peat soils, and subsoil extracts (Hansen et al., 2016; Olshansky et al., 2018; Zhang et al., 2022)

3.4 PARAFAC modeling

The contour plots of the 4 components determined by PARAFAC analysis are shown in supplementary material 4. Components C1 to C4 were identified from the literature and successfully matched in the OpenFluor database with similarity scores above 0.97. Component C1 showed two excitation maxima, a first one at ≤ 240 nm and a second one with lower intensity at 320 nm with an emission maxima at 420 nm. The component C1 has been described as terrestrial DOM degraded from lignin (Peleato et al., 2018) typical of soils and terrestrial sources in aquatic environments (Garcia et al., 2018; Yamashita et al., 2021). This component has further been attributed to bioavailable organic matter, microbially derived and/or sensitive to photodegradation (Cawley et al., 2012; Eder et al., 2022). Component C2 showed an excitation maxima at ≤ 240 and a lower intensity one at 390 nm with a maximum emission intensity at 510 nm. Previous studies have reported the component C2 as an ubiquitous terrestrial material with high molecular weight (MW) and aromatic content (Cawley et al., 2012; Wünsch et al., 2018; Yamashita et al., 2021). It has also been reported as fluorophores derived from higher plants and associated with photochemical (Coulson et al., 2022; Eder et al., 2022) or microbial (Cory and McKnight, 2005) degradation. Component C3 showed an excitation maximum at 365 nm and an emission at 443 nm. It has been reported to be high MW, aromatic and hydrophobic molecules, corresponding to lignin-like compounds (Dainard et al., 2015; Derrien et al., 2018; Rinot et al., 2021). Other studies reported component C3 as organic matter of plant origin that has undergone little transformation in the soil after production (Catalá et al., 2021; Retelletti Brogi et al., 2019). Finally, the component C4 showed an excitation maximum at 280 nm and an emission at 330 nm. Numerous studies have reported this component to be attributed to amino acids, either free or bound to proteins, or to phenolic-type compounds (Coble, 1996; Kida et al., 2019; Parlanti et al., 2000; Wauthy et al., 2018).

Of the four components identified, only component C4 showed a decreasing trend during the incubation experiment (Figure 5). Indeed, for both soil extracts, the maximum fluorescence intensity of the C4 component decreased significantly (Tukey test, $p < 0.05$, n=50), from 2.6 ± 0.3 ± to 0.8 ± 0.2 for the forest soil extracts and from 1.9 ± 0.7 to 0.5 ± 0.1 for the vineyard soil extracts. On the other hand, all components showed significant differences between streams adjacent to the forest sampled during high and low water periods. In these samples, component C1 varied between 0.62 ± 0.1 and 0.97 ± 0.19 R.U, C2 between 0.34 ± 0.06 and 0.58 ± 0.11 R.U, component C3 between 0.22 ± 0.03 and 0.34 ± 0.06 R.U and component C4 varied between 0.10 ± 0.02 and 0.16 ±0.01 R.U.

3.5 Size exclusion chromatography and Gaussian decomposition

The HPSEC/UV-fluorescence chromatograms provided additional information on the size distribution of DOM molecules contained in the samples. The Gaussian decomposition of the chromatograms revealed 6 to 8 fractions, depending on wavelength detection, distributed throughout the chromatogram. The percentage contribution of the LMW fraction (Section 2.5.4), for UV detection at 254 nm (Figure 6.A) and fluorescence at 280-330 and 278-354 nm (Figure 6.C, D), was significantly higher, before incubation, in forest soil extracts compared to vineyard soil extracts (Tukey test, $p < 0.05$, n=50). At the end of the experiment, the percentage of LMW was different only for UV detection at 254 nm (Tukey test, $p < 0.05$, n=50). For the adjacent water streams, significant differences were observed on the 280-330 and 278-354 nm fluorescence ranges according to the low vs. high water hydrological regime and this for both soil occupations (Figure 6.C,D). The MMW fraction, which corresponds to all Gaussian components classified between 1 kDa and 10 kDa, showed the least variation. Nevertheless, the percentage of MMW at UV 254 nm were significantly different between the two types of soil extracts at the end of the incubation period (Tukey test, $p < 0.05$, n=50). The HMW fraction (> 10 kDa) showed very low percentages (< 10 %) compared to the LMW and MMW fractions

for UV detection at 254 nm and fluorescence at 315-443 nm (figure 6B). However, the HMW fraction was higher for 280-330 and 278-354 nm fluorescence detection with a significant difference (Tukey test, $p < 0.05$, n=50) between forest and vineyard soil extracts before incubation. For adjacent streams, the HMW fraction was also present at very low percentages and no difference was observed between soil occupations nor beteween low and high water regimes.

4 Discussion

4.1 Incubation experiment: from labile to refractory DOM in soil extracts

In the natural environment, the labile fraction of DOM is mainly degraded in the soil before being transported to the adjacent stream. Thus, the incubation experiment was designed to remove a possible labile fraction of DOM in the soil extracts before comparison with DOM from adjacent streams. During the 28-day incubation, most of the DOC mass was lost in the first 3 days for both soils (Figure 2A). The percentage of DOC loss stabilized between 40 and 70 % after 3 days incubation. These results are consistent with those obtained in previous studies investigating the biodegradation of water-extracted DOM from different soil types such as forest, pasture and agricultural soils (Guigue et al., 2014; Kalbitz et al., 2003). DOC loss ismostly explained by the degradation of labile DOM that is easily assimilated by microorganisms. It is well known that certain organic molecules, such as amino acids or carboxylic acids, are considered as labile while other molecules, such as lignins, are considered more recalcitrant (Eilers et al., 2010). The variability of the percentage of DOC loss observed in this study (between 40 and 70 %) could be explained by differences in the microorganisms communities contained in the soil samples. Indeed, it has been shown that a greater diversity of microorganisms in soils favors the DOC degradation (Raczka et al., 2021). Different proportions of labile and recalcitrant DOM pools in the soils could also explain the variability of DOC loss. Thus, soils containing higher levels of labile DOM will be degraded to a greater proportion than soils containing high levels of refractory DOM.

The degradation of labile molecules induced an increase in the average aromaticity content, average size and molecular weight of molecules, as highlighted by the indicators $SUVA_{254}$, E2.E3 and SR. Previous studies have also shown that degraded organic matter has relatively higher aromaticity content and molecular weight (Guarch-Ribot and Butturini, 2016; Hansen et al., 2016). The E3.E4 indicator being inversely correlated to the humification of DOM (Claret

et al., 2003) can be interpreted with the HIX indicator. The HIX and E3.E4 indicators show that the degree of humification of soil extracts was low at the beginning of incubation, and then increased to stabilize after 3 days of incubation for vineyard soils. For forest soils, a gradual increase was observed throughout the incubation period until 28 days where a significant decrease occurred. The unexpected decrease observed for forest soil extracts at the end of incubation could be explained by the very high values of γ band (280-330 nm); linked with protein-like compounds. The HIX index corresponds to the ratio of areas 435-480 nm and 300-345 nm of the emission spectrum for an excitation at 255 nm, thus a high γ band intensity can make the HIX values vary drastically. The other explanation could come from the humic fraction of forest soils. Indeed, it is a complex fraction consisting of functional groups such as phenols, quinones, methoxyls and carbonyls (Maccarthy, 2001), that are recalcitrant with a slow kinetic of degradation due to its complex chemical nature (Marschner et al., 2008). Humification is a process of DOM condensation resulting from several interactions such as plant alteration with partially degraded lignins or the transformation of polyphenols, amino acids and some sugars into quinones under the enzymatic action of microorganisms (Stevenson, 1995). This slow process can sometimes take years.

The BIX index showed a significant variability in forest soil extracts contrary to vineyard soils. This could be explained by a more contrasted biological activity in forest soil extracts than in vineyard soils. Based on the hypothesis that biological activity is directly related to the diversity of microbial communities, vineyard soil extracts may have less microbial diversity due to intensive soil exploitation allowing an homogenization of the communities present in the soil (Jangid et al., 2008). Other studies mention the concept of "priming effect", which reflects a greater mineralization of organic matter in soils enriched with fresh litter(Derrien et al., 2019). This could be the case for forest soils which are subject to a contribution of fresh organic matter through vegetation cover. In addition, the significant decrease of the YFI indicator shows a

lower contribution of protein-like compounds at the end of the experiment. EEM fluorescence and PARAFAC decomposition bring details on the nature of the degraded molecules along the incubation. The component C4 (275-350) allows to affirm that some degraded labile molecules are tryptophan-like with recent biological production (Fellman et al., 2008). No significant difference was observed in the evolution of the other components C1, C2 and C3 which are characteristic of the following typical compounds: terrestrial humic-like (plant derived), humic-like matter, commonly found in agricultural catchments and terrestrial high aromatic and hydrophobic macromolecules (Derrien et al., 2018; Jørgensen et al., 2011; Rinot et al., 2021). It has been reported in previous studies that the degraded molecules are generally low molecular weight compounds (Fujii et al., 2010; Ondrasek et al., 2019). However, the size exclusion chromatography showed a decrease in the contribution of low molecular weight molecules LMW< 1k Da, and also high molecular weight macromolecules HMW > 10 kDa at the same time. Based on these results, protein-like content of DOM is likely to be composed of both LMW and HMW fractions. The fraction of medium molecular weight (MMW) compounds, linked to C1, C2 and C3 PRAFAC components (lignin compounds and terrestrial derived DOM), did not vary significantly and seemed to be recalcitrant and not easily degradable.

4.2 Evolution of DOM characteristics from soils to adjacent streams

The evolution of soil extracted DOM during the incubation experiment in comparison with the adjacent watercourse DOM is shown in the the principal component analysis (PCA), plotted with the 26 optical indicators calculated from UV-Visible, EEM fluorescence and HPSEC/UV-fluorescence (Figure 7). The PCA shows that the optical fingerprints of forest and vineyard soil extracts are more distinct at the end of incubation experiment (82 dats) than before. . This could be explained by the nature and the proportion of labile vs refractory fractions of DOM before and after incubation. This suggests that the labile fraction of DOM is not so different between the two soil types. For all indicators, the evolution of DOM optical fingerprints during the

incubation tends towards that of adjacent watercourse (Figure 7). The adjacent stream samples show relatively high contribution of medium weighted molecules MMW and a lower contribution of both low and high molecules of the protein and humic types (LMW and HMW). This could be explained by the fact that watercourse DOM has already undergone mineralization processes, mainly through microorganisms in top soil layers, before it reaches the adjacent watercourses. Other abiotic ways such as photodegradation and adsorption can influence DOM composition, which can explain the observed differences between samples at the end of incubation and the adjacent watercourse samples. The PCA also showed that water samples taken downstream of the forest soils seem more heterogeneous than downstream of the vineyard soils, whatever the hydrological regime. This heterogeneity could be explained by in-situ complex abiotic processes as well as by the difference in vegetation cover in the Ardières-Morcille watershed. Indeed, the forest sources considered in this study are mostly influenced by coniferous forests, but broad-leaved forests and natural grasslands can represent up to 35% of the total sub-catchment areas (calculation based on land use maps, CLC 2018). A previous study highlighted different DOM quality between deciduous and coniferous forests (Thieme et al., 2019). On the contrary, the viticultural sub-catchments are very homogeneous in terms of vegetation cover as they are subject to strict local regulations. The hydrologic regime also seems to have an influence on DOM quality especially for vineyard adjacent watercourses. This could be explained by the contribution of an autochthonous source being more heightened during low water periods. Autochthonous DOM is essentialy produced locally by the microbial activities (Münster, 1993) and it was demonstrated previously that there is an impact of agriculture on increasing carbon and nutrient inputs to downstream watercourses (Williams et al., 2010). These nutrient inputs provide energy support for microbial activity which can affect DOM quantity and quality.

4.3 How do the fingerprints match between DOM in soil extracts after incubation and that in downstream watercourses during high and low water periods?

As discussed in the previous section, hydrological regime influences the quantity and quality of the DOM in the watercourses. It is therefore more appropriate to look for markers of forest and vineyard soils downstream of the waterways draining these soils considering both high and low water sampling periods. To do this, a linear discriminant analysis (LDA) was applied in two steps. In a first step, the construction of the LDA 1 was conducted with 3 groups: i) a first group, called Forest DOM HW (high water), containing samples of degraded forest soils and adjacent forest streams collected at high water. ii) A second group, called Vineyard DOM HW, which contained samples of degraded vineyard soils with water from adjacent vineyard streams collected at high water, and iii) a third group called low water samples, which contained all the samples from adjacent watercourses taken during low water periods. The purpose of the first LDA (Figure 8.A) was to identify if there was similarities between DOM markers from soil extracts and DOM from the adjacent watercourse during high water period. In a second step, a LDA 2 was carried out by reversing the groups of water samples, thus considering i) a first group Forest DOM LW (low water), which contained the samples of forest soil extracts and forest adjacent watercourses taken during low water. ii) a second group of Vineyard DOM LW with samples from degraded vineyard soils and low water vineyard watercourses; and iii) a third group of high water samples containing all the samples of the adjacent watercourses taken during high water. The second LDA (Figure 8.B) was conducted to determine any similarities between soil extracts and adjacent watercourses during low water periods.

Among the 26 optical indicators (UV-Visible, EEM fluorescence and HPSEC/UV-fluorescence) considered in this study, 6 indicators were able to correctly classify the samples into Forest DOM HW, Vineyard DOM HW and Low water samples groups (Figure 8). They correspond to one UV-Visible indicator (slope ratio SR), two EEM fluorescence indicators

517 (HIX and PARAFAC component C1) and three HPSEC/UV-fluorescence indicators (LMW-
518 TSA 254, MMW TSF 278-354 and MMW TSF 280-330). The results from LDA 2 also allowed
519 the selection of 6 indicators that classified the samples into Forest DOM LW, Vineyard DOM
520 LW and High water samples groups (Figure 8.B). There were one UV-Visible indicator
521 ($SUVA_{254}$), three EEM fluorescence indicators (HIX, FI and YFI) and two HPSEC/UV-
522 fluorescence indicators (MMW TSF 278-354 and MMW TSF 280-330). Through this
523 supervised cross-sectional analysis, we have highlighted a series of indicators of terrigenous
524 contribution in both high water and low water periods. These results reveal that: (i) there is an
525 influence of land use on the quality of DOM in adjacent streams using selected optical
526 indicators, and (ii) this influence is present as well in periods of high water as in periods of low
527 water. During high water, DOM sampled downstream of forest soils comprise of relatively
528 lower molecular weight compounds with low degrees of humification and higher contribution
529 of protein-type molecules smaller than 1000 Da. On the contrary, the vineyard DOM carries a
530 higher molecular weight, ahigher degree of humification and a lower contribution of small
531 protein-type molecules. During the low water period, DOM sampled downstream of the forest
532 soils has higher aromaticity and molecular weight than the vineyard DOM which contains
533 relatively low molecules. Indeed, vinayard DOM could beimpacted by higher microbial
534 activity (Chavarria et al., 2021; Williams et al., 2010). The differences observed between DOM
535 sampled downstream forest and vineyard regardless the hydrological conditions can be
536 explained by several mechanisms. First, the presence of a biodegraded form of DOM in
537 vineyard soils probably due to the intensive exploitation of the soils and the low rooting
538 networks. Indeed, previous studies reported an higher organic matter oxidation in agricutural
539 soils which are more prone to erosion than forest soils and to an accelerated phenomenon of
540 open-air oxidation in the upper soil layers (Graeber et al., 2012; Shang et al., 2018).Secondly,
541 given the very steep slopes that favore surface runoff in the Ardières-Morcille watershed, the

542 differences observed between high and low water could be explained by a contribution of
543 surface soil organic matter during high water and a contribution of deeper and more degraded
544 soil organic matter during low water period.

545 It is important to note that DOM fingerprints presented in this study are not generalizable to
546 other watersheds. Considerable differences can be observed from one watershed to another
547 depending on topography, flow direction and soil characteristics. However, the fingerprints of
548 DOM sampled in a stream downstream of a homogeneous watershed while accounting for
549 hydrologic conditions provides a good representation of land use type. This sampling method
550 can be applied to other land use types with different agricultural and livestock types and
551 pressures. Moreover, given the complexity of DOM composition and reactivity, the
552 combination of optical indicators was essential. The result of the LDA, when calculated with
553 UV-Visible, EEM fluroescence and HPSEC/UV-fluorescence indicators separately, could not
554 provide a good differenciation between forest and vineyard DOM (Supplementary Material 5).
555 At last, indicators from HPSEC/UV-fluorescence proposed in this study, have shown potential
556 as good markers of diffuse sources of DOM in streams as discussed more in depth in the next
557 part 4.4 .

558 **4.4 Relevance of HPSEC/UV-fluorescence indicators to study DOM**

559 The HPSEC/UV-fluorescence indicators presented in this study provided additional
560 information regarding classical optical proxies (Table 1). For example, the SUVA indicator
561 highlight the aromatic content of DOM and the LMW TSA 254 indicator reflects the
562 contribution of molecules lower than 1 k Da (Supplementary Material 6). A negative correlation
563 (Pearson test, $p< 0.05$, $n=70$) between the two indicators demonstrates that the low molecular
564 weight compounds detected at 254 nm are poorly aromatic and that the aromatic content of
565 DOM is mostly found in compounds larger than 1 k Da. The correlation matrix (Supplementary

Material 6) also shows that the indicator HMW TSF 280-330 is positively correlated with the component PARAFAC C4 associated with protein-like compounds. This suggests that the C4 component is composed of relatively large molecules (> 10 k Da). In the context of this study, this showed that DOM labile pool was also composed of high molecular weight compounds in contrast to what has been reported in previous studies (Curtis-Jackson et al., 2009; Derrien et al., 2019). Other indicators of HPSEC/UV-fluorescence (e.g. HMW TSF 278-354) point out the limitations of using classic indicators like slope ratio SR indicator (Table 1). Indeed, in some soil extract , the SR indicator showed the presence of DOM mostly consisting of low molecular weight compounds, while the HMW TSF 278-354 indicator showed a relatively high contribution of amino-acid type compounds larger than 10 k Da. This result suggests that the SR indicator could be limited to the description of certain types of molecules that exclude acid-amine like compounds. Finaly, the indicators from HPSEC/UV-fluoresecence could be use a larger scale like in monitoring studies of agricultural, industrial and urban discharges. The information provided by these indicators would allow better identification of anthropogenic compounds (e.g. pesticides, pharmaceuticals) that are very complicated to detect using classical optical proxies as most of these compounds have almost similar optical properties (Hassoun et al., 2017). Also, the establishment of databases of HPSEC/UV-fluorescence indicators specific to anthropogenic compounds of interest, could facilitate their detection at lower cost than with current techniques using chromatography coupled with mass spectrometry.

5 Conclusion

The objective of this study was to provide insight into the sampling of terrigenous diffuse sources of DOM directly into streams using relevant land use markers. These markers were identified by comparing DOM from soil extracts with adjacent watercourse DOM, sampled at the outlet of homogenous sub-catchments during low and high water.

The UV-Visible, EEM fluorescence and HPSEC/UV-fluorescence techniques showed an evolution of DOM extracted from forest and vineyard soils during a 28-day incubation experiment. Indicators calculated from these techniques showed that the evolution of DOM mainly occurred in the three first days of incubation.This resulted in the degradation of high (>10 k Da) and low (<1 k Da) MW protein-like molecules (labile fraction of DOM), leading to an increase of aromaticity and humification mostly observed in medium molecular weight compounds (from 1 to 10 k Da). The labile fraction of DOM did not differ according to the land use.

Adjacent stream samples had distinct optical fingerprints influenced mostly by the hydrological regime, as DOM sampled during high water periods showed a large contribution of LMW and HMW than DOM sampled during low water periods. At the end of the incubation study, forest and vineyard soil extract tend to fingerprints of the adjacent watercourse samples. Linear discriminant analysis (LDA) revealed the relevance of 9 indicators to differentiate forest DOM and vineyard DOM fingerprints during high and low water sampling. These results demonstrate that a representative sampling of a diffuse source of DOM in rivers should take into account both the homogeneity of the upstream sub-catchments in terms of land use but also the hydrological conditions. The cross exploitation of the data from these three techniques seems appropriate to establish DOM fingerprints. However, the fingerprints of forest and vineyard diffuse sources studied in this work are not exhaustive contrary to the methodological approach,

609 which can be applicable to other types of diffuse sources. Indeed, application of this approach
610 on a larger scale would provide specific fingerprints for terrigenous diffuse sources in streams.

Acknowledgements

This study was part of the "CHYPSTER" project supported by the French National Research Agency (ANR-21-CE34-0013-01) and "IDESOC" project granted by Zone Atelier Bassin du Rhône (ZABR) and Rhône Méditerranée Corse Water Agency (AERMC). The authors wish to acknowledge Loïc Richard and Alexandra Gruat for their assistance in field sampling, samples preparation and chemical analysis.

Credit Author Statement

Amine Boukra: Conceptualization, Methodology, Software, Investigation, Formal analysis, Data curation, Writing original draft, Visualization. **Matthieu Masson**: Conceptualization, Writing-review and editing, Supervision, Project administration, Funding acquisition. **Corinne Brosse:** Resources. **Mahaut Sourzac** : Resources. **Edith Parlanti**: Software, Writing-review and editing, Resources. **Cécile Miege**: Conceptualization, Writing-review and editing, Supervision, Project administration, Funding acquisition.

References

Aiken, G.R., 2014. 1.11 - Dissolved Organic Matter in Aquatic Systems, in: Ahuja, S. (Ed.), Comprehensive Water Quality and Purification. Elsevier, Waltham, pp. 205–220. https://doi.org/10.1016/B978-0-12-382182-9.00014-1

Asmala, E., Massicotte, P., Carstensen, J., 2021. Identification of dissolved organic matter size components in freshwater and marine environments. Limnol. Oceanogr. 66, 1381–1393. https://doi.org/10.1002/lno.11692

Berg, S.M., Whiting, Q.T., Herrli, J.A., Winkels, R., Wammer, K.H., Remucal, C.K., 2019. The Role of Dissolved Organic Matter Composition in Determining Photochemical Reactivity at the Molecular Level. Environ. Sci. Technol. 53, 11725–11734. https://doi.org/10.1021/acs.est.9b03007

Bolan, N.S., Adriano, D.C., Kunhikrishnan, A., James, T., McDowell, R., Senesi, N., 2011. Chapter One - Dissolved Organic Matter: Biogeochemistry, Dynamics, and Environmental Significance in Soils, in: Sparks, D.L. (Ed.), Advances in Agronomy. Academic Press, pp. 1–75. https://doi.org/10.1016/B978-0-12-385531-2.00001-3

Brezinski, K., Gorczyca, B., 2019. An overview of the uses of high performance size exclusion chromatography (HPSEC) in the characterization of natural organic matter (NOM) in potable water, and ion-exchange applications. Chemosphere 217, 122–139. https://doi.org/10.1016/j.chemosphere.2018.10.028

Carstea, E.M., Popa, C.L., Baker, A., Bridgeman, J., 2020. In situ fluorescence measurements of dissolved organic matter: A review. Sci. Total Environ. 699, 134361. https://doi.org/10.1016/j.scitotenv.2019.134361

Catalá, T.S., Shorte, S., Dittmar, T., 2021. Marine dissolved organic matter: a vast and unexplored molecular space. Appl. Microbiol. Biotechnol. 105, 7225–7239. https://doi.org/10.1007/s00253-021-11489-3

Cawley, K.M., Ding, Y., Fourqurean, J., Jaffé, R., 2012. Characterising the sources and fate of dissolved organic matter in Shark Bay, Australia: a preliminary study using optical properties and stable carbon isotopes. Mar. Freshw. Res. 63, 1098. https://doi.org/10.1071/MF12028

Chavarria, K.A., Saltonstall, K., Vinda, J., Batista, J., Lindmark, M., Stallard, R.F., Hall, J.S., 2021. Land use influences stream bacterial communities in lowland tropical watersheds. Sci. Rep. 11, 21752. https://doi.org/10.1038/s41598-021-01193-7

Claret, F., Schäfer, T., Bauer, A., Buckau, G., 2003. Generation of humic and fulvic acid from Callovo-Oxfordian clay under high alkaline conditions. Sci. Total Environ. 317, 189–200. https://doi.org/10.1016/S0048-9697(03)00337-1

Coble, P.G., 1996. Characterization of marine and terrestrial DOM in seawater using excitation-emission matrix spectroscopy. Mar. Chem. 51, 325–346. https://doi.org/10.1016/0304-4203(95)00062-3

Cory, R.M., McKnight, D.M., 2005. Fluorescence Spectroscopy Reveals Ubiquitous Presence of Oxidized and Reduced Quinones in Dissolved Organic Matter. Environ. Sci. Technol. 39, 8142–8149. https://doi.org/10.1021/es0506962

Coulson, L.E., Weigelhofer, G., Gill, S., Hein, T., Griebler, C., Schelker, J., 2022. Small rain events during drought alter sediment dissolved organic carbon leaching and respiration

675 in intermittent stream sediments. Biogeochemistry 159, 159–178.
676 https://doi.org/10.1007/s10533-022-00919-7

677 Curtis-Jackson, P.K., Massé, G., Gledhill, M., Fitzsimons, M.F., 2009. Characterization of
678 low molecular weight dissolved organic nitrogen by liquid chromatography-
679 electrospray ionization-mass spectrometry. Limnol. Oceanogr. Methods 7, 52–63.
680 https://doi.org/10.4319/lom.2009.7.52

681 Dainard, P.G., Guéguen, C., McDonald, N., Williams, W.J., 2015. Photobleaching of
682 fluorescent dissolved organic matter in Beaufort Sea and North Atlantic Subtropical
683 Gyre. Mar. Chem. 177, 630–637. https://doi.org/10.1016/j.marchem.2015.10.004

684 Derrien, M., Kim, M.-S., Ock, G., Hong, S., Cho, J., Shin, K.-H., Hur, J., 2018. Estimation of
685 different source contributions to sediment organic matter in an agricultural-forested
686 watershed using end member mixing analyses based on stable isotope ratios and
687 fluorescence spectroscopy. Sci. Total Environ. 618, 569–578.
688 https://doi.org/10.1016/j.scitotenv.2017.11.067

689 Derrien, M., Shin, K.-H., Hur, J., 2019. Biodegradation-induced signatures in sediment pore
690 water dissolved organic matter: Implications from artificial sediments composed of
691 two contrasting sources. Sci. Total Environ. 694, 133714.
692 https://doi.org/10.1016/j.scitotenv.2019.133714

693 Eder, A., Weigelhofer, G., Pucher, M., Tiefenbacher, A., Strauss, P., Brandl, M., Blöschl, G.,
694 2022. Pathways and composition of dissolved organic carbon in a small agricultural
695 catchment during base flow conditions. Ecohydrol. Hydrobiol. 22, 96–112.
696 https://doi.org/10.1016/j.ecohyd.2021.07.012

697 Eilers, K.G., Lauber, C.L., Knight, R., Fierer, N., 2010. Shifts in bacterial community
698 structure associated with inputs of low molecular weight carbon compounds to soil.
699 Soil Biol. Biochem.

700 Fellman, J.B., D'Amore, D.V., Hood, E., Boone, R.D., 2008. Fluorescence characteristics and
701 biodegradability of dissolved organic matter in forest and wetland soils from coastal
702 temperate watersheds in southeast Alaska. Biogeochemistry 88, 169–184.
703 https://doi.org/10.1007/s10533-008-9203-x

704 Fujii, K., Hayakawa, C., Van Hees, P.A.W., Funakawa, S., Kosaki, T., 2010. Biodegradation
705 of low molecular weight organic compounds and their contribution to heterotrophic
706 soil respiration in three Japanese forest soils. Plant Soil 334, 475–489.
707 https://doi.org/10.1007/s11104-010-0398-y

708 Garcia, R.D., Diéguez, M. del C., Gerea, M., Garcia, P.E., Reissig, M., 2018. Characterisation
709 and reactivity continuum of dissolved organic matter in forested headwater catchments
710 of Andean Patagonia. Freshw. Biol. 63, 1049–1062.
711 https://doi.org/10.1111/fwb.13114

712 Gouy, V., Liger, L., Ahrouch, S., Bonnineau, C., Carluer, N., Chaumot, A., Coquery, M.,
713 Dabrin, A., Margoum, C., Pesce, S., 2021. Ardières-Morcille in the Beaujolais,
714 France: A research catchment dedicated to study of the transport and impacts of
715 diffuse agricultural pollution in rivers. Hydrol. Process. 35, e14384.
716 https://doi.org/10.1002/hyp.14384

717 Graeber, D., Gelbrecht, J., Pusch, M.T., Anlanger, C., von Schiller, D., 2012. Agriculture has
718 changed the amount and composition of dissolved organic matter in Central European

719 headwater streams. Sci. Total Environ. 438, 435–446.
720 https://doi.org/10.1016/j.scitotenv.2012.08.087

721 Guarch-Ribot, A., Butturini, A., 2016. Hydrological conditions regulate dissolved organic
722 matter quality in an intermittent headwater stream. From drought to storm analysis.
723 Sci. Total Environ. 571, 1358–1369. https://doi.org/10.1016/j.scitotenv.2016.07.060

724 Guigue, J., Mathieu, O., Lévêque, J., Mounier, S., Laffont, R., Maron, P.-A., Navarro, N.,
725 Chateau-Smith, C., Suchet, P., Lucas, Y., 2014. A comparison of extraction
726 procedures for water-extractable organic matter in soils. Eur. J. Soil Sci. 65, 520–530.
727 https://doi.org/10.1111/ejss.12156

728 Hansen, A.M., Kraus, T.E.C., Pellerin, B.A., Fleck, J.A., Downing, B.D., Bergamaschi, B.A.,
729 2016. Optical properties of dissolved organic matter (DOM): Effects of biological and
730 photolytic degradation. Limnol. Oceanogr. 61, 1015–1032.
731 https://doi.org/10.1002/lno.10270

732 Hassoun, H., Lamhasni, T., Foudeil, S., El Bakkali, A., Ait Lyazidi, S., Haddad, M.,
733 Choukrad, M., Hnach, M., 2017. Total Fluorescence Fingerprinting of Pesticides: A
734 Reliable Approach for Continuous Monitoring of Soils and Waters. J. Fluoresc. 27,
735 1633–1642. https://doi.org/10.1007/s10895-017-2100-8

736 Hawkes, J.A., Sjöberg, P.J.R., Bergquist, J., Tranvik, L.J., 2019. Complexity of dissolved
737 organic matter in the molecular size dimension: insights from coupled size exclusion
738 chromatography electrospray ionisation mass spectrometry. Faraday Discuss. 218, 52–
739 71. https://doi.org/10.1039/C8FD00222C

740 Helms, J.R., Stubbins, A., Ritchie, J.D., Minor, E.C., Kieber, D.J., Mopper, K., 2008.
741 Absorption spectral slopes and slope ratios as indicators of molecular weight, source,
742 and photobleaching of chromophoric dissolved organic matter. Limnol. Oceanogr. 53,
743 955–969. https://doi.org/10.4319/lo.2008.53.3.0955

744 Heo, J., Yoon, Y., Kim, D.-H., Lee, H., Lee, D., Her, N., 2016. A new fluorescence index
745 with a fluorescence excitation-emission matrix for dissolved organic matter (DOM)
746 characterization. Desalination Water Treat. 57, 20270–20282.
747 https://doi.org/10.1080/19443994.2015.1110719

748 Huang, Y., Du, Y., Ma, T., Deng, Y., Tao, Y., Xu, Y., Leng, Z., 2021. Dissolved organic
749 matter characterization in high and low ammonium groundwater of Dongting Plain,
750 central China. Ecotoxicol. Environ. Saf. 208, 111779.
751 https://doi.org/10.1016/j.ecoenv.2020.111779

752 Huguet, A., Vacher, L., Relexans, S., Saubusse, S., Froidefond, J.-M., Parlanti, E., 2009.
753 Properties of fluorescent dissolved organic matter in the Gironde Estuary. Org.
754 Geochem. 40, 706–719. https://doi.org/10.1016/j.orggeochem.2009.03.002

755 Jaffé, R., Boyer, J.N., Lu, X., Maie, N., Yang, C., Scully, N.M., Mock, S., 2004. Source
756 characterization of dissolved organic matter in a subtropical mangrove-dominated
757 estuary by fluorescence analysis. Mar. Chem. 84, 195–210.
758 https://doi.org/10.1016/j.marchem.2003.08.001

759 Jangid, K., Williams, M.A., Franzluebbers, A.J., Sanderlin, J.S., Reeves, J.H., Jenkins, M.B.,
760 Endale, D.M., Coleman, D.C., Whitman, W.B., 2008. Relative impacts of land-use,
761 management intensity and fertilization upon soil microbial community structure in
762 agricultural systems. Soil Biol. Biochem. 40, 2843–2853.
763 https://doi.org/10.1016/j.soilbio.2008.07.030

764 Jørgensen, L., Stedmon, C.A., Kragh, T., Markager, S., Middelboe, M., Søndergaard, M.,
765 2011. Global trends in the fluorescence characteristics and distribution of marine
766 dissolved organic matter. Mar. Chem. 126, 139–148.
767 https://doi.org/10.1016/j.marchem.2011.05.002

768 Kalbitz, K., Schmerwitz, J., Schwesig, D., Matzner, E., 2003. Biodegradation of soil-derived
769 dissolved organic matter as related to its properties. Geoderma, Ecological aspects of
770 dissolved organic matter in soils 113, 273–291. https://doi.org/10.1016/S0016-
771 7061(02)00365-8

772 Kida, M., Kojima, T., Tanabe, Y., Hayashi, K., Kudoh, S., Maie, N., Fujitake, N., 2019.
773 Origin, distributions, and environmental significance of ubiquitous humic-like
774 fluorophores in Antarctic lakes and streams. Water Res. 163, 114901.
775 https://doi.org/10.1016/j.watres.2019.114901

776 Li, P., Hur, J., 2017. Utilization of UV-Vis spectroscopy and related data analyses for
777 dissolved organic matter (DOM) studies: A review. Crit. Rev. Environ. Sci. Technol.
778 47. https://doi.org/10.1080/10643389.2017.1309186

779 Maccarthy, P., 2001. The Principles of Humic Substances. Soil Sci. 166, 738–751.
780 https://doi.org/10.1097/00010694-200111000-00003

781 Marschner, B., Brodowski, S., Dreves, A., Gleixner, G., Gude, A., Grootes, P.M., Hamer, U.,
782 Heim, A., Jandl, G., Ji, R., Kaiser, K., Kalbitz, K., Kramer, C., Leinweber, P.,
783 Rethemeyer, J., Schäffer, A., Schmidt, M.W.I., Schwark, L., Wiesenberg, G.L.B.,
784 2008. How relevant is recalcitrance for the stabilization of organic matter in soils? J.
785 Plant Nutr. Soil Sci. 171, 91–110. https://doi.org/10.1002/jpln.200700049

786 Massicotte, P., Markager, S., 2016. Using a Gaussian decomposition approach to model
787 absorption spectra of chromophoric dissolved organic matter. Mar. Chem. 180, 24–32.
788 https://doi.org/10.1016/j.marchem.2016.01.008

789 Mcknight, D., Boyer, E., Westerhoff, P., Doran, P., Kulbe, T., Andersen, D., 2001.
790 Spectrofluorometric Characterization of Dissolved Organic Matter for Indication of
791 Precursor Organic Material and Aromaticity. Limnol. Oceanogr. 46, 38–48.
792 https://doi.org/10.4319/lo.2001.46.1.0038

793 Michael-Kordatou, I., Michael, C., Duan, X., He, X., Dionysiou, D.D., Mills, M.A., Fatta-
794 Kassinos, D., 2015. Dissolved effluent organic matter: Characteristics and potential
795 implications in wastewater treatment and reuse applications. Water Res. 77, 213–248.
796 https://doi.org/10.1016/j.watres.2015.03.011

797 Mladenov, N., Parsons, D., Kinoshita, A.M., Pinongcos, F., Mueller, M., Garcia, D., Lipson,
798 D.A., Grijalva, L.M., Zink, T.A., 2022. Groundwater-surface water interactions and
799 flux of organic matter and nutrients in an urban, Mediterranean stream. Sci. Total
800 Environ. 811, 152379. https://doi.org/10.1016/j.scitotenv.2021.152379

801 Münster, U., 1993. Concentrations and fluxes of organic carbon substrates in the aquatic
802 environment. Antonie Van Leeuwenhoek 63, 243–274.
803 https://doi.org/10.1007/BF00871222

804 Murphy, K.R., Stedmon, C.A., Graeber, D., Bro, R., 2013. Fluorescence spectroscopy and
805 multi-way techniques. PARAFAC. Anal. Methods 5, 6557–6566.
806 https://doi.org/10.1039/C3AY41160E

807 Nebbioso, A., Piccolo, A., 2013. Molecular characterization of dissolved organic matter
808 (DOM): a critical review. Anal. Bioanal. Chem. 405, 109–124.
809 https://doi.org/10.1007/s00216-012-6363-2

810 Olshansky, Y., Root, R.A., Chorover, J., 2018. Wet–dry cycles impact DOM retention in
811 subsurface soils. Biogeosciences 15, 821–832. https://doi.org/10.5194/bg-15-821-2018

812 Ondrasek, G., Bakić Begić, H., Zovko, M., Filipović, L., Meriño-Gergichevich, C., Savić, R.,
813 Rengel, Z., 2019. Biogeochemistry of soil organic matter in agroecosystems &
814 environmental implications. Sci. Total Environ. 658, 1559–1573.
815 https://doi.org/10.1016/j.scitotenv.2018.12.243

816 Parlanti, E., Wörz, K., Geoffroy, L., Lamotte, M., 2000. Dissolved organic matter
817 fluorescence spectroscopy as a tool to estimate biological activity in a coastal zone
818 submitted to anthropogenic inputs. Org. Geochem. 31, 1765–1781.
819 https://doi.org/10.1016/S0146-6380(00)00124-8

820 Peleato, N.M., Legge, R.L., Andrews, R.C., 2018. Neural networks for dimensionality
821 reduction of fluorescence spectra and prediction of drinking water disinfection by-
822 products. Water Res. 136, 84–94. https://doi.org/10.1016/j.watres.2018.02.052

823 Peyrard, X., Liger, L., Guillemain, C., Gouy, V., 2016. A trench study to assess transfer of
824 pesticides in subsurface lateral flow for a soil with contrasting texture on a sloping
825 vineyard in Beaujolais. Environ. Sci. Pollut. Res. 23, 14–22.
826 https://doi.org/10.1007/s11356-015-4917-5

827 Rabiet, M., Coquery, M., Carluer, N., Gahou, J., Gouy, V., 2015. Transfer of metal(loid)s in a
828 small vineyard catchment: contribution of dissolved and particulate fractions in river
829 for contrasted hydrological conditions. Environ. Sci. Pollut. Res. 22, 19224–19239.
830 https://doi.org/10.1007/s11356-015-5079-1

831 Raczka, N.C., Piñeiro, J., Tfaily, M.M., Chu, R.K., Lipton, M.S., Pasa-Tolic, L., Morrissey,
832 E., Brzostek, E., 2021. Interactions between microbial diversity and substrate
833 chemistry determine the fate of carbon in soil. Sci. Rep. 11, 19320.
834 https://doi.org/10.1038/s41598-021-97942-9

835 Retelletti Brogi, S., Derrien, M., Hur, J., 2019. In-Depth Assessment of the Effect of Sodium
836 Azide on the Optical Properties of Dissolved Organic Matter. J. Fluoresc. 29, 877–
837 885. https://doi.org/10.1007/s10895-019-02398-w

838 Reuter, J.H., Perdue, E.M., 1977. Importance of heavy metal-organic matter interactions in
839 natural waters. Geochim. Cosmochim. Acta 41, 325–334.
840 https://doi.org/10.1016/0016-7037(77)90240-X

841 Rinot, O., Borisover, M., Levy, G.J., Eshel, G., 2021. Fluorescence spectroscopy: A sensitive
842 tool for identifying land-use and climatic region effects on the characteristics of water-
843 extractable soil organic matter. Ecol. Indic. 121, 107103.
844 https://doi.org/10.1016/j.ecolind.2020.107103

845 Sanderman, J., Lohse, K.A., Baldock, J.A., Amundson, R., 2009. Linking soils and streams:
846 Sources and chemistry of dissolved organic matter in a small coastal watershed. Water
847 Resour. Res. 45. https://doi.org/10.1029/2008WR006977

848 Schwarz, G., 1978. Estimating the Dimension of a Model. Ann. Stat. 6, 461–464.

849 Shang, P., Lu, Y., Du, Y., Jaffé, R., Findlay, R.H., Wynn, A., 2018. Climatic and watershed
850 controls of dissolved organic matter variation in streams across a gradient of

agricultural land use. Sci. Total Environ. 612, 1442–1453. https://doi.org/10.1016/j.scitotenv.2017.08.322

Stevenson, F.J., 1995. Humus Chemistry: Genesis, Composition, Reactions, Second Edition. J. Chem. Educ. 72, A93. https://doi.org/10.1021/ed072pA93.6

Thieme, L., Graeber, D., Hofmann, D., Bischoff, S., Schwarz, M.T., Steffen, B., Meyer, U.-N., Kaupenjohann, M., Wilcke, W., Michalzik, B., Siemens, J., 2019. Dissolved organic matter characteristics of deciduous and coniferous forests with variable management: different at the source, aligned in the soil. Biogeosciences 16, 1411–1432. https://doi.org/10.5194/bg-16-1411-2019

Verkh, Y., Rozman, M., Petrovic, M., 2018. Extraction and cleansing of data for a non-targeted analysis of high-resolution mass spectrometry data of wastewater. MethodsX 5, 395–402. https://doi.org/10.1016/j.mex.2018.04.008

Wauthy, M., Rautio, M., Christoffersen, K.S., Forsström, L., Laurion, I., Mariash, H.L., Peura, S., Vincent, W.F., 2018. Increasing dominance of terrigenous organic matter in circumpolar freshwaters due to permafrost thaw. Limnol. Oceanogr. Lett. 3, 186–198. https://doi.org/10.1002/lol2.10063

Weishaar, J.L., Aiken, G.R., Bergamaschi, B.A., Fram, M.S., Fujii, R., Mopper, K., 2003. Evaluation of Specific Ultraviolet Absorbance as an Indicator of the Chemical Composition and Reactivity of Dissolved Organic Carbon. Environ. Sci. Technol. 37, 4702–4708. https://doi.org/10.1021/es030360x

Williams, C.J., Frost, P.C., Morales-Williams, A.M., Larson, J.H., Richardson, W.B., Chiandet, A.S., Xenopoulos, M.A., 2016. Human activities cause distinct dissolved organic matter composition across freshwater ecosystems. Glob. Change Biol. 22, 613–626. https://doi.org/10.1111/gcb.13094

Williams, C.J., Yamashita, Y., Wilson, H.F., Jaffé, R., Xenopoulos, M.A., 2010. Unraveling the role of land use and microbial activity in shaping dissolved organic matter characteristics in stream ecosystems. Limnol. Oceanogr. 55, 1159–1171. https://doi.org/10.4319/lo.2010.55.3.1159

Wünsch, U.J., Geuer, J.K., Lechtenfeld, O.J., Koch, B.P., Murphy, K.R., Stedmon, C.A., 2018. Quantifying the impact of solid-phase extraction on chromophoric dissolved organic matter composition. Mar. Chem. 207, 33–41. https://doi.org/10.1016/j.marchem.2018.08.010

Yamashita, Y., Kojima, D., Yoshida, N., Shibata, H., 2021. Relationships between dissolved black carbon and dissolved organic matter in streams. Chemosphere 271, 129824. https://doi.org/10.1016/j.chemosphere.2021.129824

Zark, M., Dittmar, T., 2018. Universal molecular structures in natural dissolved organic matter. Nat. Commun. 9, 1–8. https://doi.org/10.1038/s41467-018-05665-9

Zhang, X., Li, Y., Ye, J., Chen, Z., Ren, D., Zhang, S., 2022. The spectral characteristics and cadmium complexation of soil dissolved organic matter in a wide range of forest lands. Environ. Pollut. 299, 118834. https://doi.org/10.1016/j.envpol.2022.118834

Zsolnay, Á., 2003. Dissolved organic matter: artefacts, definitions, and functions. Geoderma, Ecological aspects of dissolved organic matter in soils 113, 187–209. https://doi.org/10.1016/S0016-7061(02)00361-0

Zsolnay, A., Baigar, E., Jimenez, M., Steinweg, B., Saccomandi, F., 1999. Differentiating with fluorescence spectroscopy the sources of dissolved organic matter in soils

subjected to drying. Chemosphere 38, 45–50. https://doi.org/10.1016/S0045-6535(98)00166-0

900 **Figures**

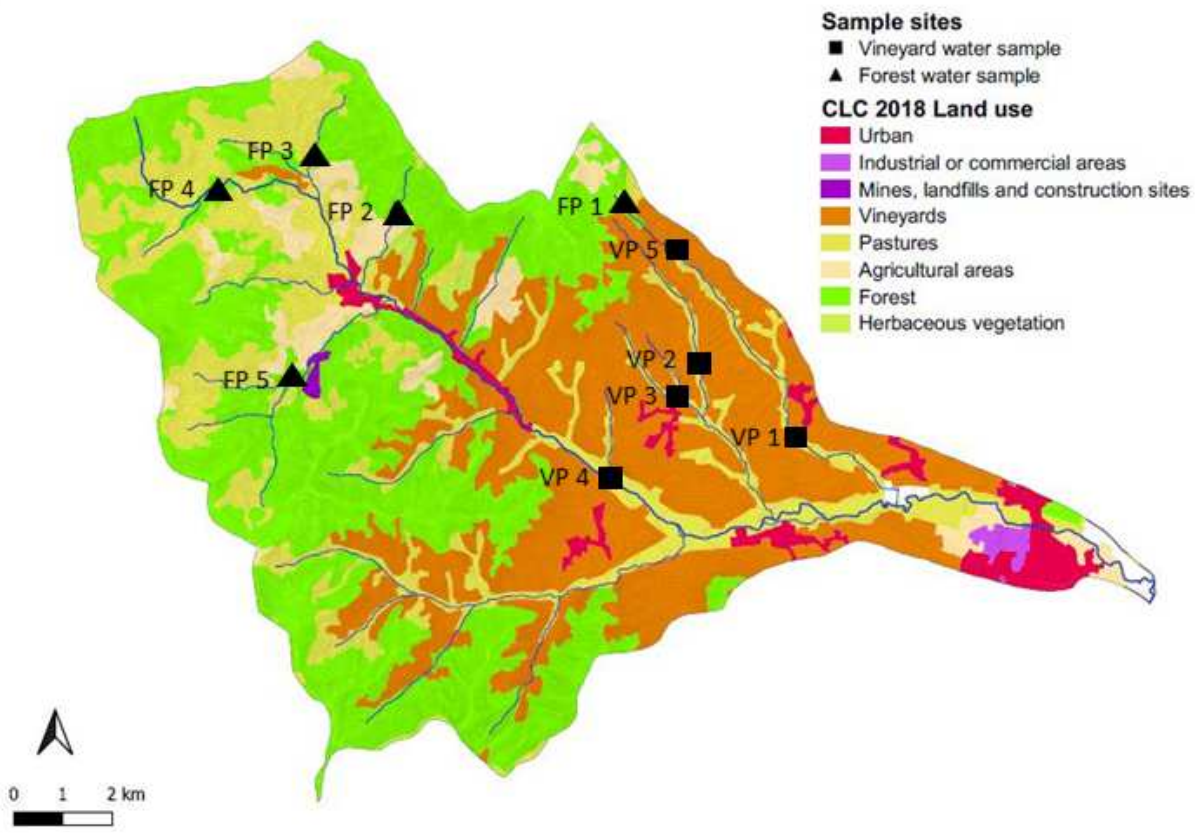

901

902

903 **Figure 1**. Map of Ardieres-Morcille catchment howing the location of the water-sampling sites
904 (FP: forest sampling points, VP: vineyard sampling points) and the land-use boundaries (Corine
905 Land Cover CLC 2018). The soil samples were collected upstream the water sampling points.

906

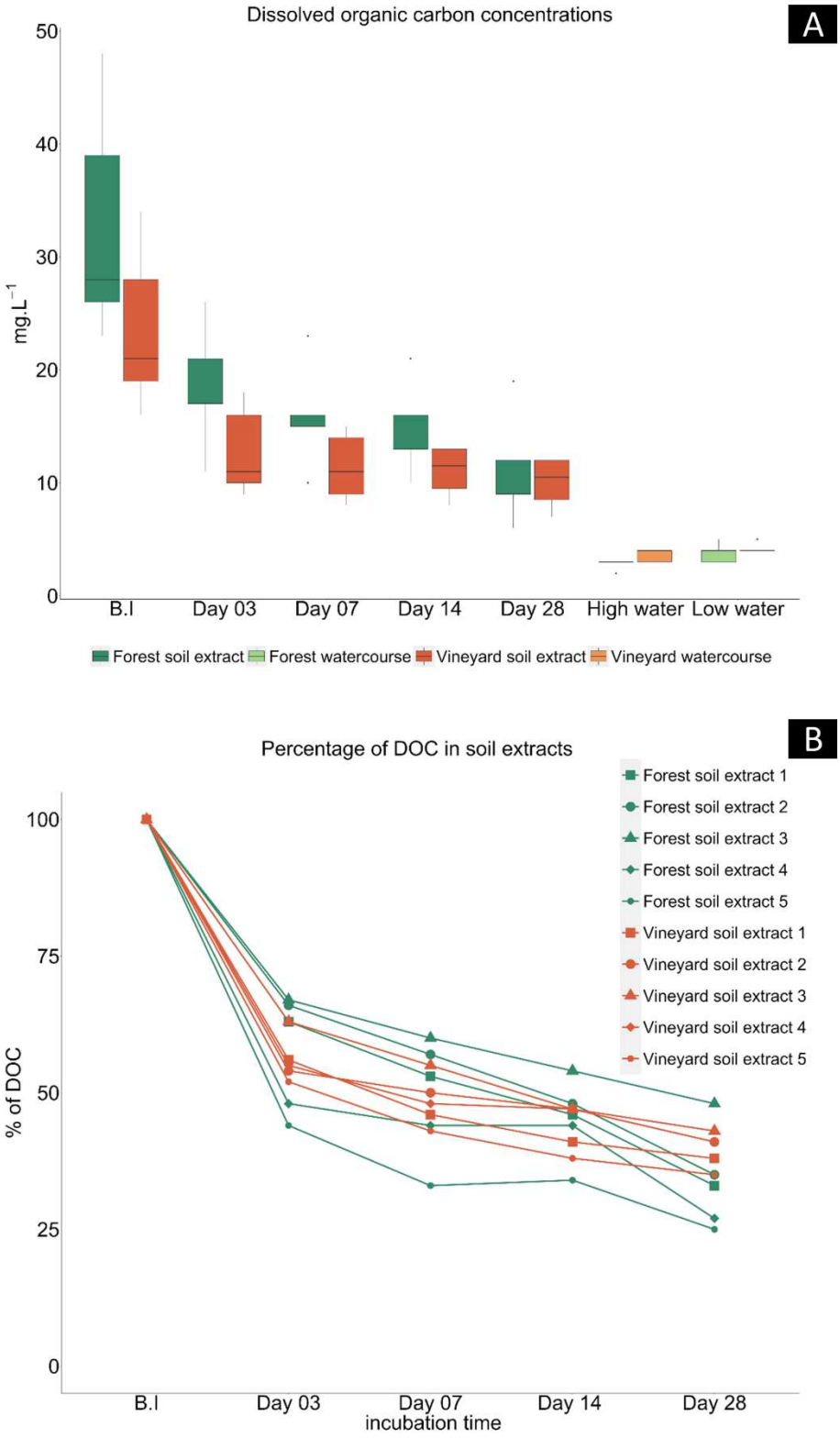

907

908 **Figure 2.** A: Dissolved organic carbon (DOC) concentrations measured i) in soil extracts (forest
909 in dark green and vineyard in dark orange) before incubation (B.I) and after 3, 7, 14 and 28
910 days of incubation, and ii) in water samples collected from streams adjacent to the forest (in
911 light green) and vineyard (in light orange) soils during high and low water periods. B:
912 Percentage of DOC for soil extracts during the 28 days incubation experiment relative to the
913 DOC concentration measured before incubation.

914

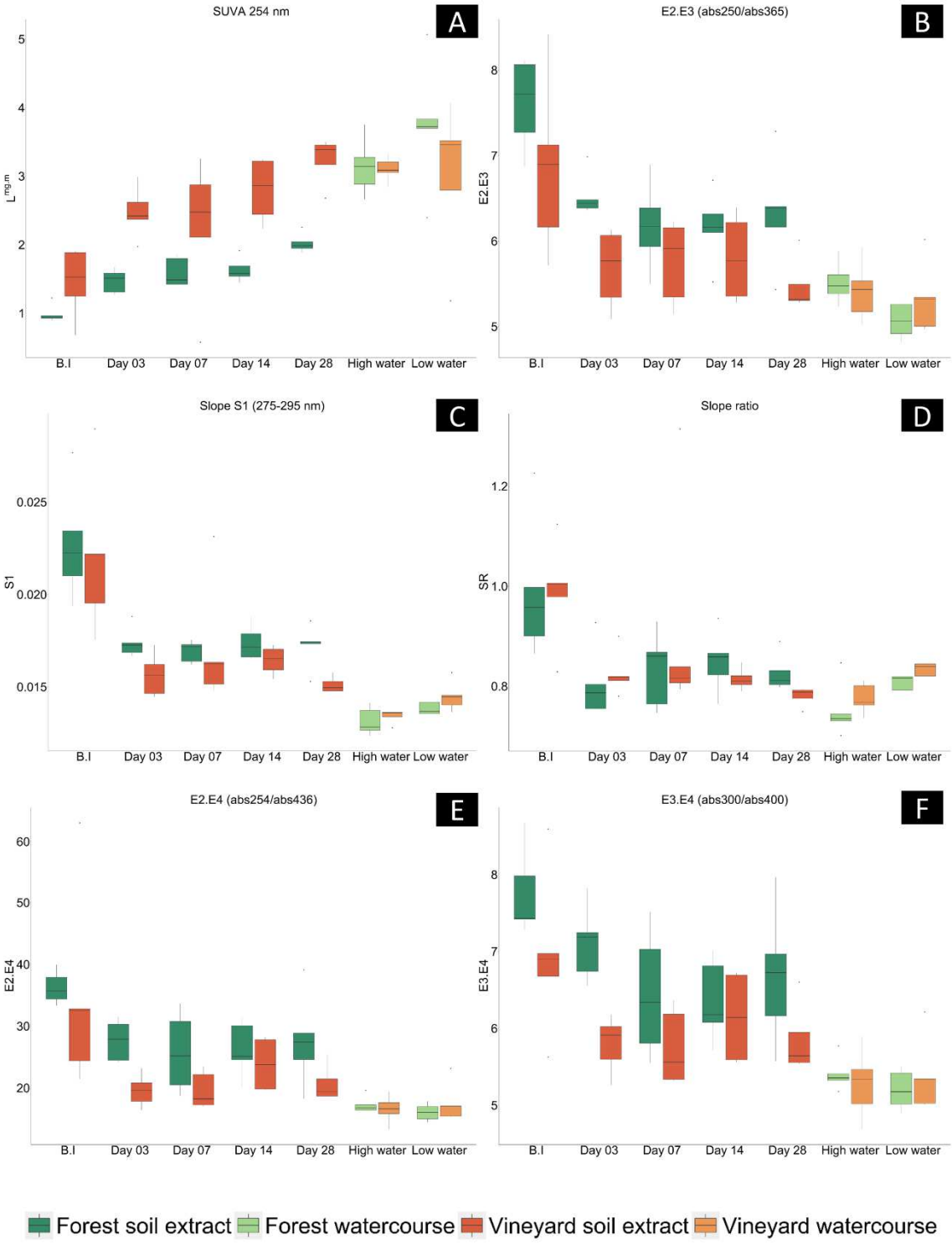

915

916 **Figure 3**. UV-Visible indicators measured i) in soil extracts (forest in dark green and vineyard
917 in dark orange) before incubation (B.I) and after 3, 7, 14 and 28 days of incubation, and ii) in
918 water samples collected from streams adjacent to the forest (in light green) and vineyard (in
919 light orange) soils during high and low water periods. A: $SUVA_{254}$, B: E2.E3 (abs250/abs365),

C: Slope S1 (275_295 nm), D: Slope ratio SR (S275_295nm/S350_400nm), E: E2.E4 (abs254/abs436) and F: E3.E4 (abs300/abs400).

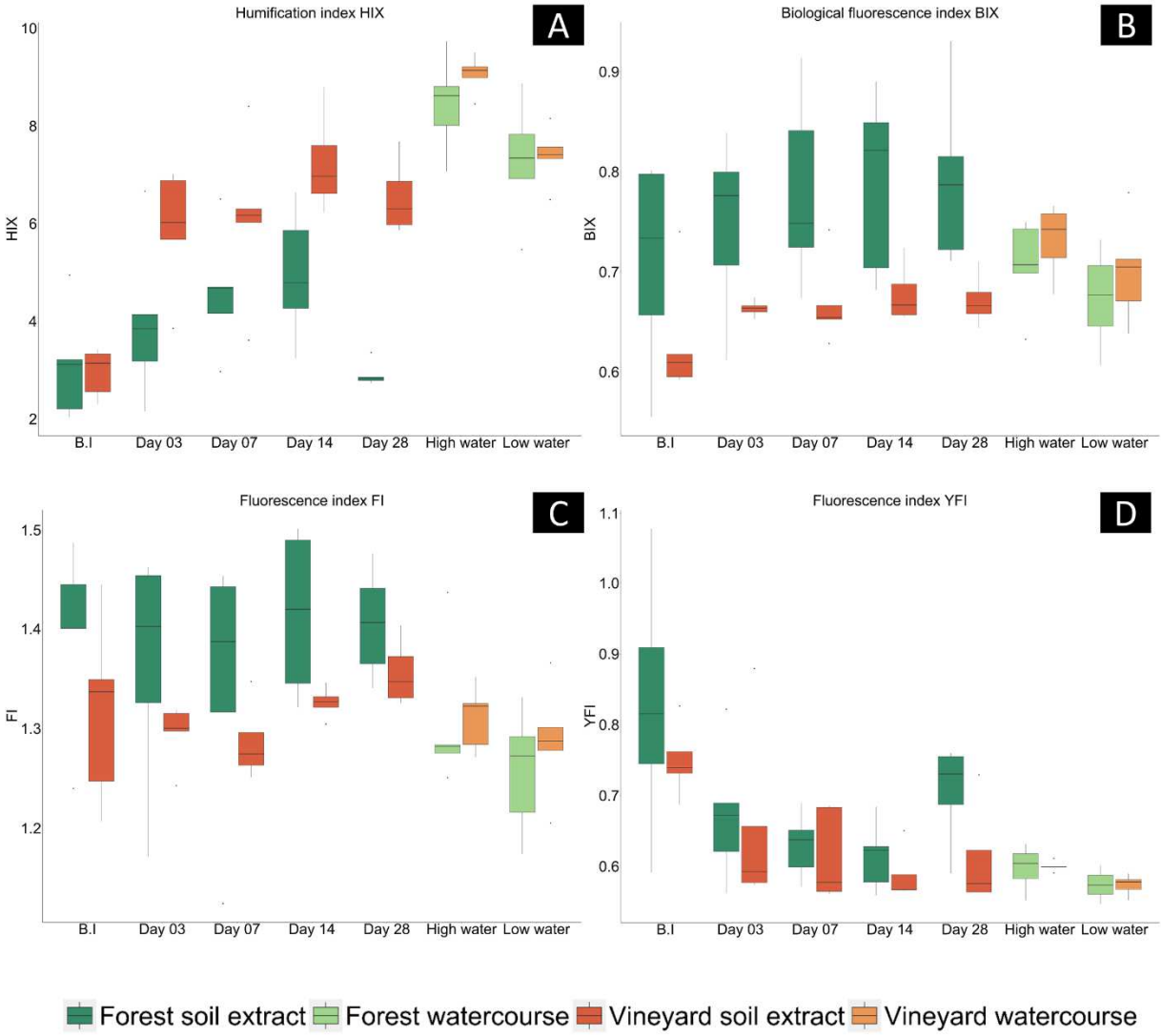

Figure 4. EEM fluorescence indicators measured i) in soil extracts (forest in dark green and vineyard in dark orange) before incubation (B.I) and after 3, 7, 14 and 28 days of incubation, and ii) in water samples collected from streams adjacent to the forest (in light green) and vineyard (in light orange) soils during high and low water periods. A: humification index HIX, B: biological fluorescence index BIX, C: fluorescence index FI and D: fluorescence index YFI.

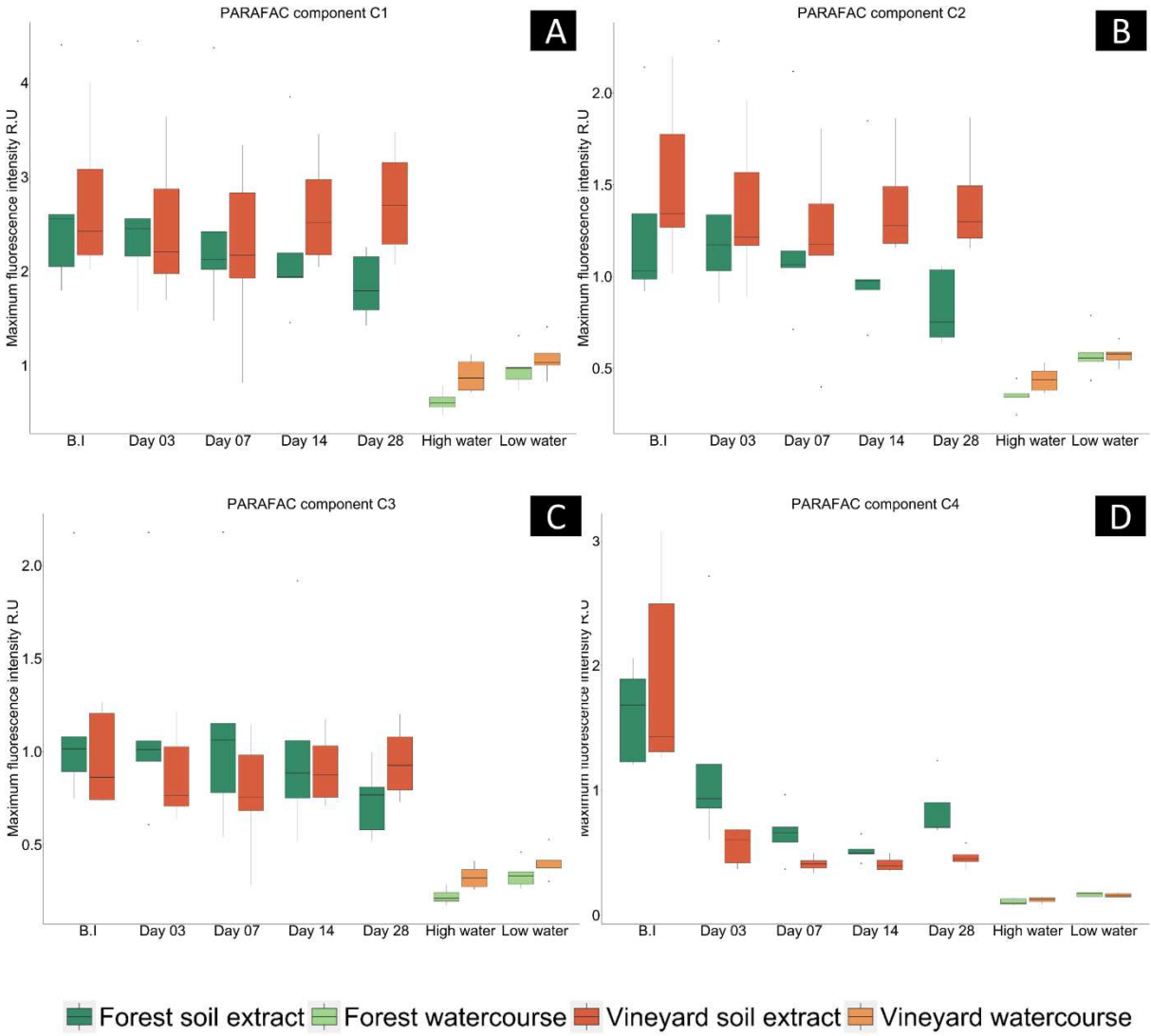

933

934

935 **Figure 5.** PARAFAC components C1 (<240(320)-420 nm), C2 (<240(390)-510 nm), C3 (365-
936 443 nm) and C4 (280-330 nm) measured i) in soil extracts (forest in dark green and vineyard in
937 dark orange) before incubation (B.I) and after at 3, 7, 14 and 28 days of incubation, and ii) in
938 water samples collected from streams adjacent to the forest (in light green) and vineyard (in
939 light orange) soils during high and low water periods.

940

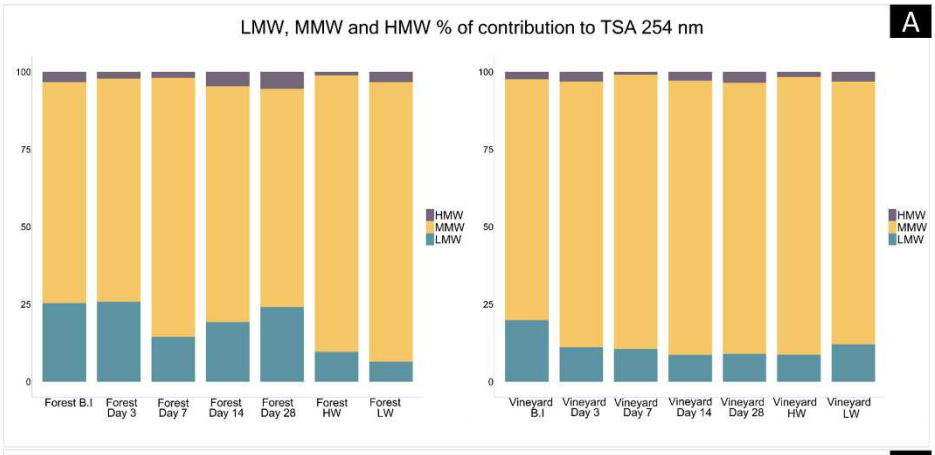
A
LMW, MMW and HMW % of contribution to TSA 254 nm
100
75
50
25
0
HMW
MMW
LMW
Forest B.I
Forest Day 3
Forest Day 7
Forest Day 14
Forest Day 28
Forest HW
Forest LW
Vineyard B.I
Vineyard Day 3
Vineyard Day 7
Vineyard Day 14
Vineyard Day 28
Vineyard HW
Vineyard LW

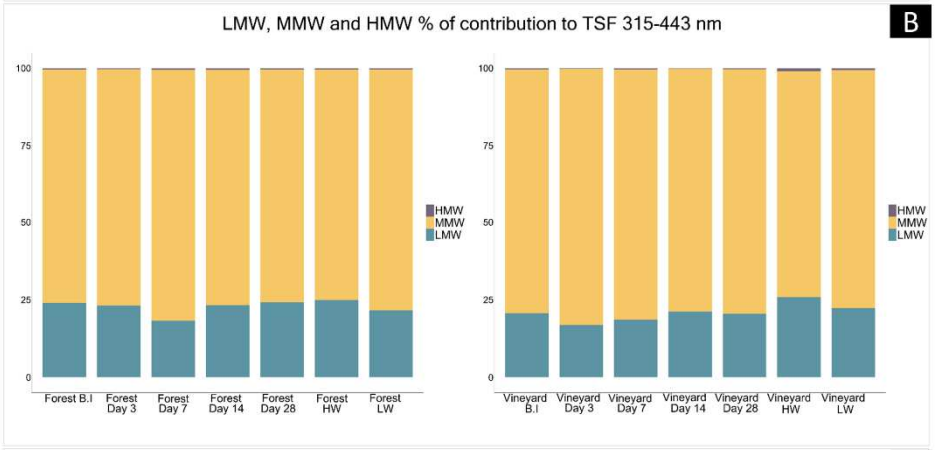
B
LMW, MMW and HMW % of contribution to TSF 315-443 nm
100
75
50
25
0
HMW
MMW
LMW
Forest B.I
Forest Day 3
Forest Day 7
Forest Day 14
Forest Day 28
Forest HW
Forest LW
Vineyard B.I
Vineyard Day 3
Vineyard Day 7
Vineyard Day 14
Vineyard Day 28
Vineyard HW
Vineyard LW

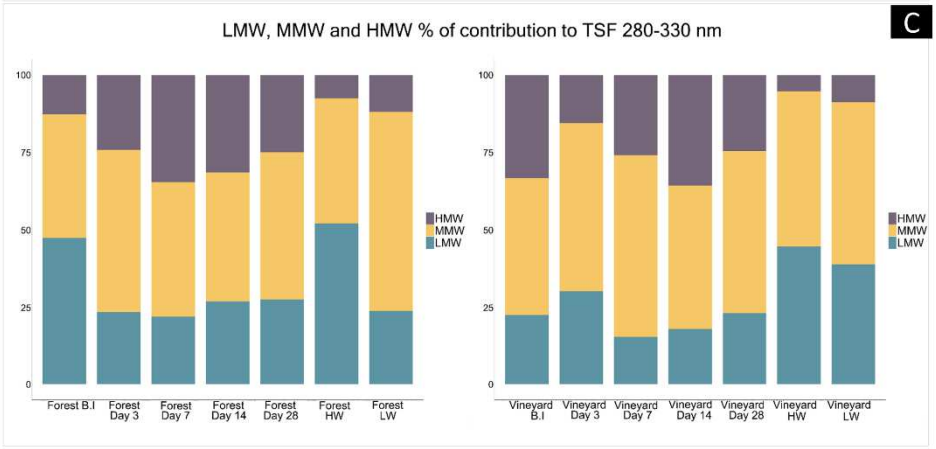
C
LMW, MMW and HMW % of contribution to TSF 280-330 nm
100
75
50
25
0
HMW
MMW
LMW
Forest B.I
Forest Day 3
Forest Day 7
Forest Day 14
Forest Day 28
Forest HW
Forest LW
Vineyard B.I
Vineyard Day 3
Vineyard Day 7
Vineyard Day 14
Vineyard Day 28
Vineyard HW
Vineyard LW

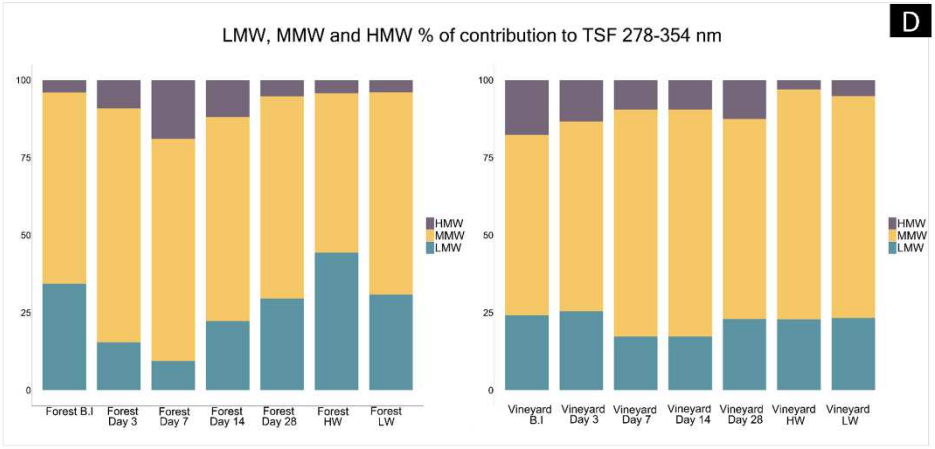
D
LMW, MMW and HMW % of contribution to TSF 278-354 nm
100
75
50
25
0
HMW
MMW
LMW
Forest B.I
Forest Day 3
Forest Day 7
Forest Day 14
Forest Day 28
Forest HW
Forest LW
Vineyard B.I
Vineyard Day 3
Vineyard Day 7
Vineyard Day 14
Vineyard Day 28
Vineyard HW
Vineyard LW

Figure 6. Low Molecular Weight (LMW; blue bars), Medium Molecular Weight (MMW; orange bars) and High Molecular Weight (HMW; purple bars) percentage of contribution to: A: Total Sec Absorbance TSA at PDA 254 nm, B: Total Sec Fluorescence TSF at Excitation Emission wavelengths 345-443 nm, C: TSF at fluorescence Excitation Emission wavelengths 280-330 nm, D: TSF at fluorescence Excitation Emission wavelengths 278-354 nm.. Samples plotted are soil extracts before incubation (B.I) and then at 3, 7, 14 and 28 days of incubation as well as for water samples collected from streams adjacent to the forest and vineyard soils during high and low water periods.

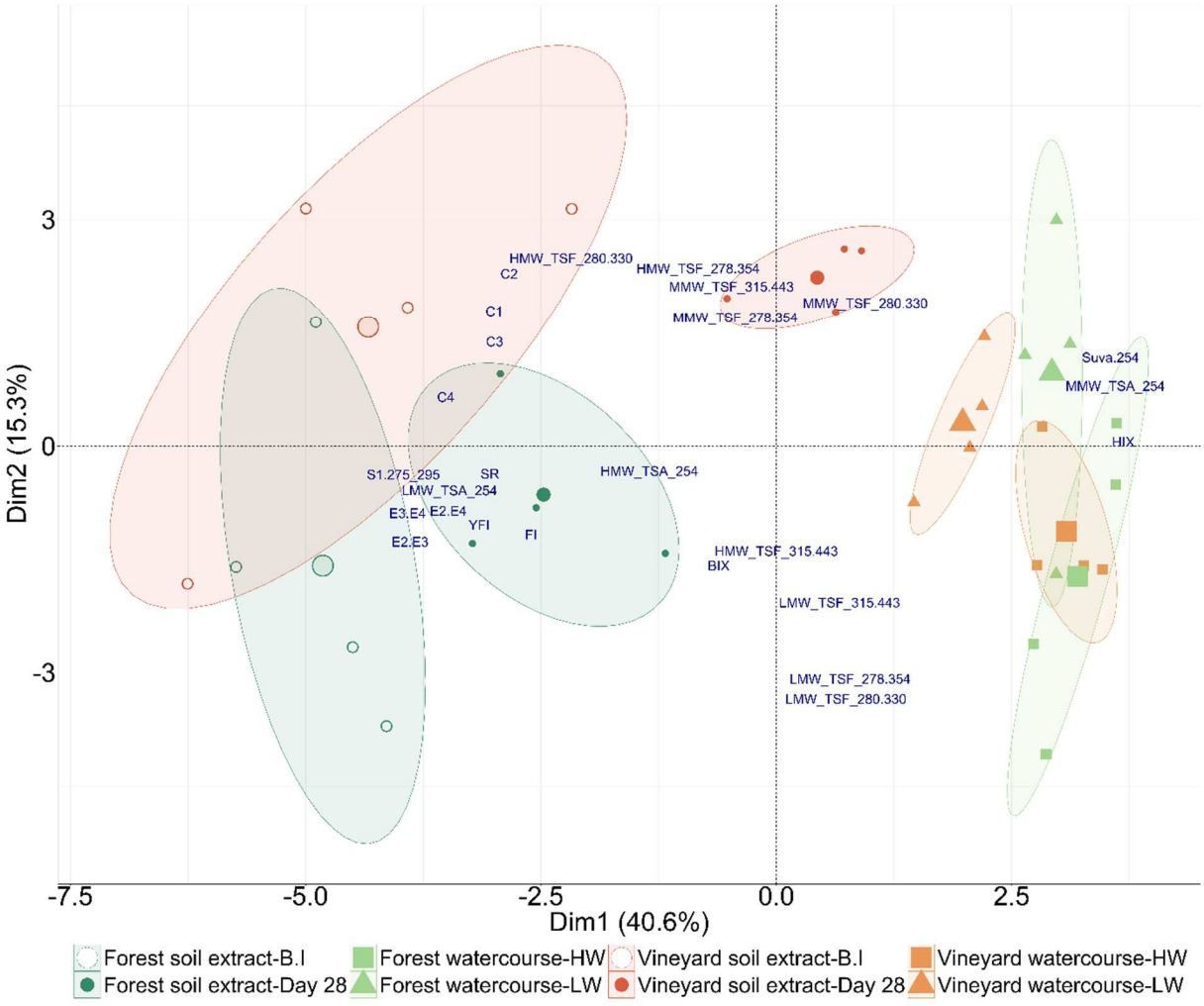

Figure 7. First factorial plane of the principal component analysis (PCA) performed on data from forest and vineyard soil extracts before incubation (B.I), after 28 days of incubation and their adjacent water stream samples collected during high and low water periods. The variables considered in the PCA are the UV-Visible, EEM fluorescence and HPSEC/UV-fluorescence indicators.

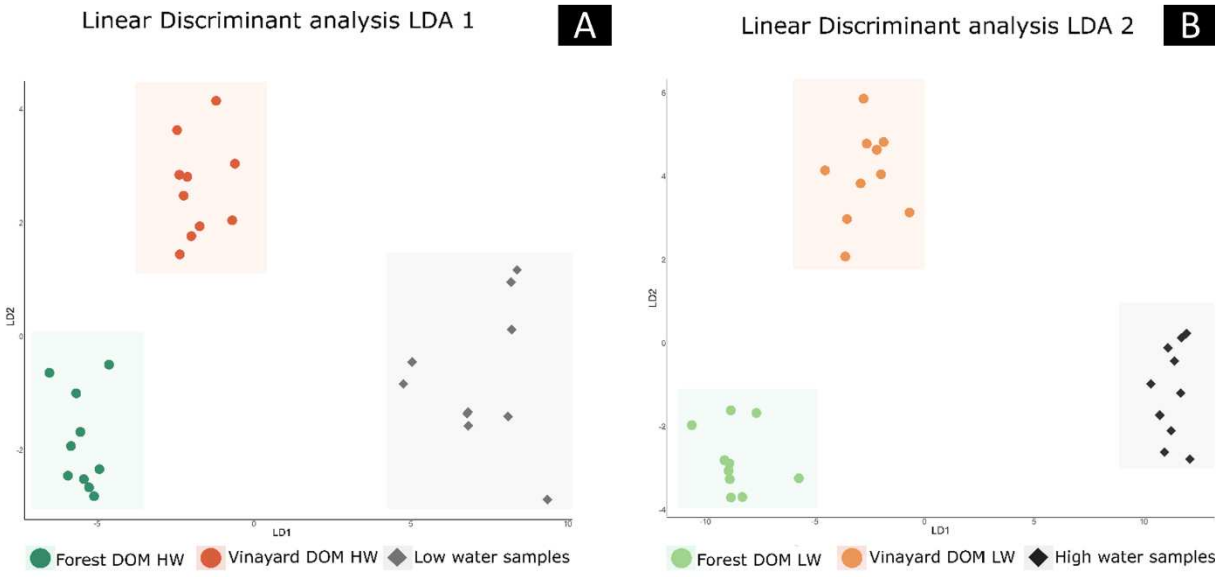

Figure 8. A. Linear discriminant analysis (LDA1) calculated with 26 indicators from UV-Visible, EEM fluorescence and HPSEC/UV-fluorescence to discriminate forest and vineyard DOM taken during high water from low water DOM. B. Linear discriminant analysis (LDA2) calculated with the same indicators to discriminate forest and vineyard DOM taken during low water periods from High water DOM.

986 **Tables**

987 Table 1. Classical UV-Visible and fluorescence indicators to characterize dissolved organic
988 matter.

Indicator	Calculation	Interpretation	References
$SUVA_{254}$	$\frac{Abs\ 254\ nm}{[DOC]}$	Correlated with the aromaticity of DOM.	(Weishaar et al., 2003)
E2.E3	$\frac{Abs\ 250\ nm}{Abs\ 365\ nm}$	Negatively correlated to organic molecules size	Helms et al., 2008
E2.E4	$\frac{Abs\ 254\ nm}{Abs\ 436\ nm}$	Autochthonous versus terrestrial DOM	Jaffé et al., 2004; Li and Hur, 2017
E3.E4	$\frac{Abs\ 300\ nm}{Abs\ 400\ nm}$	Negatively correlated to humification degree	Claret et al., 2003; Li and Hur, 2017
S_1 (275-295 nm)	$\alpha_\lambda = \alpha_{\lambda 0} e^{S(\lambda 0 - \lambda)}$ α_λ: absorption coefficient at specific wavelength $\lambda 0$: reference wavelength S: exponential slope	Negatively correlated to aromatic carbon content	Stedmon et al., 2000 Helms et al., 2008
S_2 (350-400 nm)			

SR	$\frac{S1}{S2}$	Negatively correlated to molecular weight	Helms et al., 2008
HIX	$\frac{\sum IF\ 435-480}{\sum IF\ 300-445}$ at 255 nm	Correlated to the aromatic cabon content/ humification degree of DOM	Zsolnay et al., 1999
BIX	$\frac{IF\ 380}{IF\ 430}$ at 310 nm	Indicator of recent autochthonous production of DOM due to biological activity	(Huguet et al., 2009)
FI	$\frac{IF\ 450}{IF\ 500}$ at 370 nm	Terrigenous vs microbial DOM	Mcknight et al., 2001
YFI	$\frac{FEI\ 350-400}{FEI\ 400-450}$ at 280 nm FEI : average fluorescence intensities	Increases the resolution of FI indicator	Heo et al., 2016

989

990